THE PRODUCTION OF ^{103}Pd AND ^{109}Cd USING PROTON IRRADIATED TANDEM ^{nat}Ag/^{nat}Ag TARGETS

CLAIRE INEZA

submitted in accordance with the requirements for the degree of

MASTER OF SCIENCE

In the subject

CHEMISTRY

at the

University of South Africa

Supervisor: Dr. C. Naidoo

Co-supervisor: Prof. M.J. Mphahlele

March 2015

DECLARATION

Student number: **51816830**

I, the undersigned, hereby declare '**The Production of ^{103}Pd and ^{109}Cd using Proton Irradiated Tandem ^{nat}Ag/^{nat}Ag Targets**' is my own original work and has not yet previously in its entirely or in part been submitted to any university for a masters degree in chemistry and that all the sources that I have used or quoted have been indicated and acknowledged by means of complete references.

.

Ms Claire INEZA

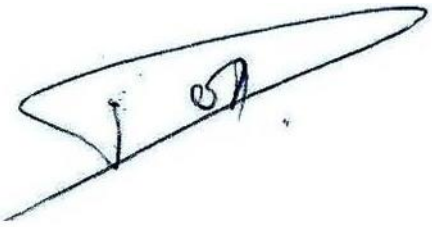

SIGNATURE DATE: **04 March 2015**

DEDICATION

This thesis is dedicated to my late father

F. KARANGWA

LIST OF FIGURES

LIST OF TABLES

ACKNOWLEDGEMENTS

There are a large number of people to whom I am deeply indebted and without whose help none of this would have been possible. Firstly, I would like to thank my supervisor, Dr Clive Naidoo, who has had the greatest influence on my fledgling scientific career. We have spent the better part of two years working together, and without his passion and tireless efforts, I would not be where I am today. I would also like to thank my co-supervisor Prof M. Jack Mphahlele at University of South Africa (UNISA) and Prof. Malik Maaza for their support.

I also had the unique opportunity to work with several people at iThemba LABS: Dr. Balla Diop Ngom, S. Zongo, and so on. A special thanks to C. Vermeulen and the Targetry team for the preparation and bombardment of the targets used in this research.

A special thanks to the Organization for Women in Science for the Developing World (OWSDW), the Swedish International Development Cooperation Agency and the National Research Foundation (NRF) for their financial support during my studies.

Most of all I would like to thank my Husband, Claude, for his ever ending love and support. My family, brother and sisters for their support, love and encouragement during the course of this project.

ABSTRACT

^{103}Pd is an important therapeutic radionuclide and has recently found great interest due to its higher radiobiologic effect. ^{109}Cd decays by electron capture and is generally used as calibration sources in industrial and medical fields. A new method for the production of ^{103}Pd and ^{109}Cd using the 66 MeV proton beam of iThemba LABS on a tandem natural silver target (Ag/Ag) has been developed. The tandem targets (each target with a mass of 9 g and a thickness of 3 mm) were placed in the high energy slot (62.515 MeV - 40.173 MeV) and low energy slot (38.652 MeV – 0 MeV) to produce the bulk ^{103}Pd and ^{109}Cd, respectively. The radiochemical separation of the Pd radionuclides (^{103}Pd, ^{100}Pd) and the co-produced Rh radioisotopes (mainly ^{101}Rh and ^{100}Rh which are produced from decay of their Pd parents) from the bulk ^{nat}Ag was achieved using a Chelex chelating resin column. In the preliminary studies, different size columns (3 cm x 1 cm, 11 cm x 1 cm, 13 cm x 1 cm and 16 cm x 1.5 cm) were investigated to determine the optimal column conditions for the separation. It was determined that the optimal conditions for the chemical separation was with a 13 cm x 1 cm resin column with the elution of Rh and Ag radionuclides carried out with 1 M HNO_3 and the elution of Pd radionuclides with 10 M HCl. No Ag or Rh impurities were detected in the final product and the average recovery of Pd was > 96 %. This work was repeated using a "hot" irradiated Ag target and the chemical processing was done in a hot cell using the same resin column conditions. The recovery of the high purity ^{103}Pd from the irradiated ^{nat}Ag target was found to be > 95 %. The radiochemical separation of ^{109}Cd from the bulk ^{nat}Ag target was done in two parts. In the first part, the precipitation method was used to reduce the silver into a metallic form using 30 g of Cu turnings. The resulting ^{109}Cd filtrate was loaded onto a AG-X10 anion exchange resin column (6 cm x 1 cm). For the optimal chemical separation, the elution of Ag and Cu(II) was carried out with 2 M HCl containing H_2O_2 and the elution of ^{109}Cd was accomplished with 1 M HNO_3. The recovery yield of ^{109}Cd was > 99 %.

Keywords:

^{103}Pd, ^{109}Cd, tandem ^{nat}Ag/^{nat}Ag target, ion exchange chromatography, Chelex-100, AG1-X10.

TABLE OF CONTENTS

Table of Contents

CHAPTER 1: INTRODUCTION

1.1 NUCLEAR SCIENCE: a historical perspective.

The discovery of radioactivity a century ago opened up a new field in science, which culminated 40 years later in the discovery of fission and its practical consequences in the form of nuclear weapons and nuclear power reactors. Nuclear science has contributed much to our daily life- it provides solutions related to health and food production as well as a means for the understanding of the universe and its composition. The discovery of the radioactivity of uranium by Herni Becquerel in February 1896 [1-3] was a direct consequence of the discovery of the X-rays by Röntgen a few months earlier who found that photographic plates were blackened in the absence of light, if they were in contact with certain minerals [3]. Two years later in 1898, many radioactive elements such as thorium [4], polonium [4,5] and radium [4] were discovered by Marie Curie and co-workers. Marchwald, on the other hand, independently discovered polonium and called it "radiotellurium" [6]. Subsequently in 1907, Campbell found that both potassium and rubidium showed a weak activity due to the emission of swift β particles [7]. In the same year, Boltwood discovered the presence of another radioactive substance in uranium minerals, which he called ionium [7]. Later on, the active form of lead called radio-lead was discovered by Hoffmann and Strauss [7]. Debierne, on the other hand, has studied a product intimately associated with thorium, which he has called actinium [8,9].

Radioactivity itself is the emission of radiation originating from a nuclear reaction or as a result of the spontaneous decay of unstable atomic nuclei. For the detection of radioactive substances, suitable detectors such as Geiger-Müller counters or photographic emulsions are needed [5]. The naturally occurring radioactive substances were the only ones available for

study until 1934 when Curie and Joliot announced that boron and aluminum could be made radioactive by process of bombardment of α-ray from polonium [10]. It was found that photographic emulsions also indicate the presence of radiation in the absence of radioactive substances. If they are shielded by thick walls of lead or other materials, the counting rate decreases appreciably. On the other hand, if the detectors are brought up to greater heights in the atmosphere, the counting rate increases to values that are higher by a factor of about 12 at a height of 9000 m above ground. This proves the presence of another kind of radiation that enters the atmosphere from outside, which is called cosmic radiation (protons, neutrons, photons, electrons, positrons, mesons) [5, 11]. The positron had been discovered only two years earlier (1932) by Anderson as a component of the cosmic radiation [5, 11, 12]. A number of laboratories quickly found that positrons could be produced in light elements by α-ray bombardment. Much earlier in 1919 Rutherford [7,12,13] had shown nuclear transmutations by α-particle bombardment, and the new phenomenon of induced radioactivity was therefore quickly understood in terms of the production of new unstable nuclei. Since then, artificial radioactivity was discovered and several laboratories had been developed and put into operation devices for the acceleration of hydrogen ions and helium ions to energies at which nuclear transmutations could occur. Furthermore, the discovery of the neutron in 1932 by Chadwick [14] and the isolation of deuterium [15] in 1933 made available two additional bombarding particles that turned out to be useful for the production of induced radioactivity. About the same time in 1931, Ernest Lawrence [16] built the first working cyclotron capable of accelerating protons, deuterons, or helium ions (alpha particles) to energies which were enough to penetrate atomic nuclei and thereby produce numerous stable and radioactive isotopes that would find many peaceful applications in improving the wellbeing of humanity all over the world. In 1940 the cyclotron developed by Lawrence and his coworkers would produce artificially as many as 223 radioactive isotopes, many of which would prove to be of immediate and immense value in medicine and biological studies. The discovery of nuclear

fission by Hahn and Strassmann gave further strong impetus to the study of new radioactive products [12]. A second major source of artificial radionuclides has become available since the development of the first successful atomic pile chain reactor in 1942. Reactor-produced radionuclides became available for public distribution since 1946 [12]. The subsequent development of nuclear reactors opened the way for their widespread applications in other fields such as chemistry, physics, biology, medicine, agriculture and engineering. Charts and tabulations of the properties of radioactive species are available [12]. So far, more than 3000 nuclides are known, of which approximately 2700 radionuclides have been artificially produced and characterized in terms of their physical properties [10].

Radionuclides have been produced in South Africa since 1965 by the Atomic Energy Corporation (AEC), now The South Africa Nuclear Energy Corporation (NECSA) [17]. The reactor-based radionuclides were produced using a 20 MW multipurpose reactor and this included the most prominent radionuclide of technetium from molybdenum targets. Accelerator-based radionuclides were produced at the Council for Scientific and Industrial Research (CSIR) cyclotron in Pretoria which decommissioned in 1988 [17]. Since then, the National Accelerator Centre (now iThemba LABS) started the routine operation of a Separated-Sector Cyclotron (SSC) for subatomic physics research, medical radiotherapy and radionuclide production. The production of short-lived radiopharmaceuticals was produced routinely in 1989 and this was supplied to more than 30 hospitals and clinics in Southern Africa. Currently, the short-lived radionuclides produced by iThemba LABS are ^{123}I, ^{67}Ga, ^{18}F and the long-lived ^{68}Ge/^{68}Ga generators. Non-medical radionuclides include the long-lived ultra-high vacuum ^{22}Na positron sources and ^{22}Na solutions. iThemba LABS still remain the only supplier of ^{22}Na positron sources in the world. A large part of the export market involves the shipment of the irradiated Rb metal targets (unprocessed material) to Canada. This accounts for more than 50% of the radionuclides sales for iThemba LABS.

Five accelerators are currently operated by iThemba LABS, four of them at the Faure facility, namely a 6 MV Van der Graaff accelerator for material science, an 8 MeV injector cyclotron providing light ions for the Separated Sector Cyclotron (SSC), a second 8 MeV injector cyclotron providing heavy ions and polarized protons for the SSC and the SSC itself. The SSC is a variable-energy machine capable of accelerating protons to a maximum energy of 200 MeV. A tandem Van der Graaff accelerator is also operated in Johannesburg at the iThemba LABS (Gauteng) facility. A layout of the SSC facility and its experimental areas is shown in Figure 1 below:

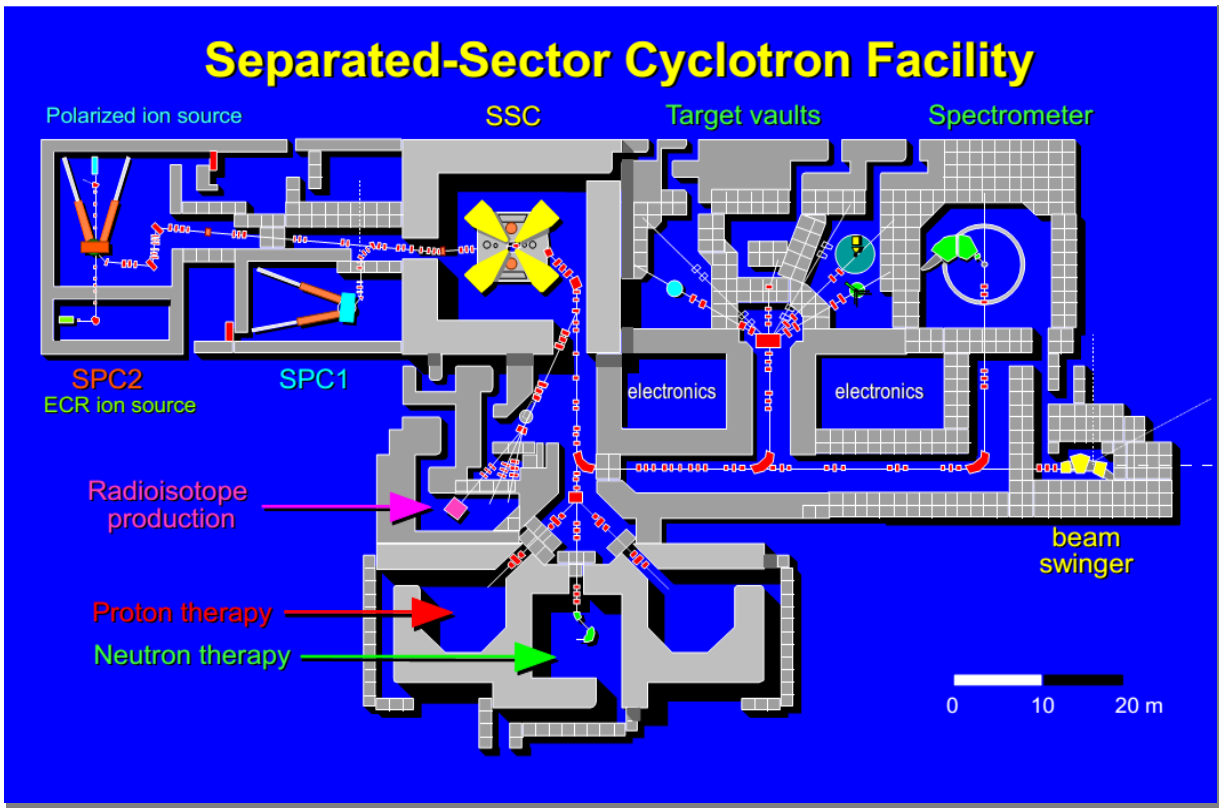

Figure 1: Separated Sector Cyclotron Facility (SSC) 200 MeV [18].

1.2 PROPERTIES AND PRODUCTION OF ^{103}Pd AND ^{109}Cd

1.2.1 Properties of ^{103}Pd and ^{109}Cd

The radionuclide ^{103}Pd has a suitable half-life of 16.96 d and decays almost exclusively by electron capture (EC) to ^{103m}Rh ($T_{1/2}$=56.1 min) resulting in the abundant emission of Auger electrons and low-energy X-rays (20-22 keV), (EC, K_{α}= 20.1 keV (64.7%), K_{β}=22.7 keV (12.3%) keV) [19,20-25]. When an inner-shell electron is removed from an atom, the vacancy will be filled by an electron from the outer shells and the excess energy will be released as a characteristic X-ray and this energy is equal to the difference between the 2 shells, or by the emission of an Auger electron and during this process the energy released by the outer shell electron is given to another electron, which then leaves the atom. The latter de-excites through a heavily converted internal transition (IT). As a result of both processes (EC and IT), X-rays (20-22 KeV) and Auger electrons (which makes this radionuclide suitable for internal radiotherapy; in every 100 decay of ^{103}Pd, 80 X-rays , 186 Auger electrons, and 95 low-energy conversion electrons are emitted) [26, 27] are emitted which are ideally suited for therapy.

Auger electrons are a third type of ionizing radiation known after alpha and beta particles. Auger electrons allow more efficient targeted radiotherapy (targeted radioimmunotherapy) with minimum damage to normal tissue due to their lower short range biological effectiveness and their high level of cytotoxicity [28]. The radionuclide is therefore being increasingly used in the treatment of prostate cancer [29] because ^{103}Pd offers a unique characteristic of pure X-ray emitter (21–23 keV) [20,30,31] and more “soft” photons. Palladium is compatible with biological tissues, practically insoluble in water and biological liquids [32] and, the chemical stability of most Pd(II) complexes is well recognized [33]. The combination

of all these properties listed above makes ^{103}Pd attractive from the dosimetry point of view [33]; a very popular treatment option in the management of early stage for prostate cancer [34] over this last decade and gives advantages of ^{103}Pd as compared with ^{125}I. This, for example, lessens the risk for the patient in case of an unforeseen source failure [32]. ^{103}Pd has more favorable physical properties, including its low energy, rapid dose fall-off, short half-life and total cumulative dose delivery at a higher dose rate than ^{125}I and is a promising radioisotope for localized tumor treatment [35]. Photon emission is largely fluorescent X-rays with an average energy of 21 keV. Two γ-rays are produced with low probability (each 0.001 per decay) and energies of 40 and 360 keV. The decay scheme can be reduced to the main electron capture transition to the 39 KeV excited level of ^{103}Rh (intensity 0.999±0.001) and a subsequent highly converted γ-transition. The emission ratio of X-rays to γ-rays is 3000 times higher [19]. These decay features of ^{103}Pd and the practical absence of high-energy γ-rays make it ideally suited for interstitial brachytherapy and its current demand is continuously increasing.

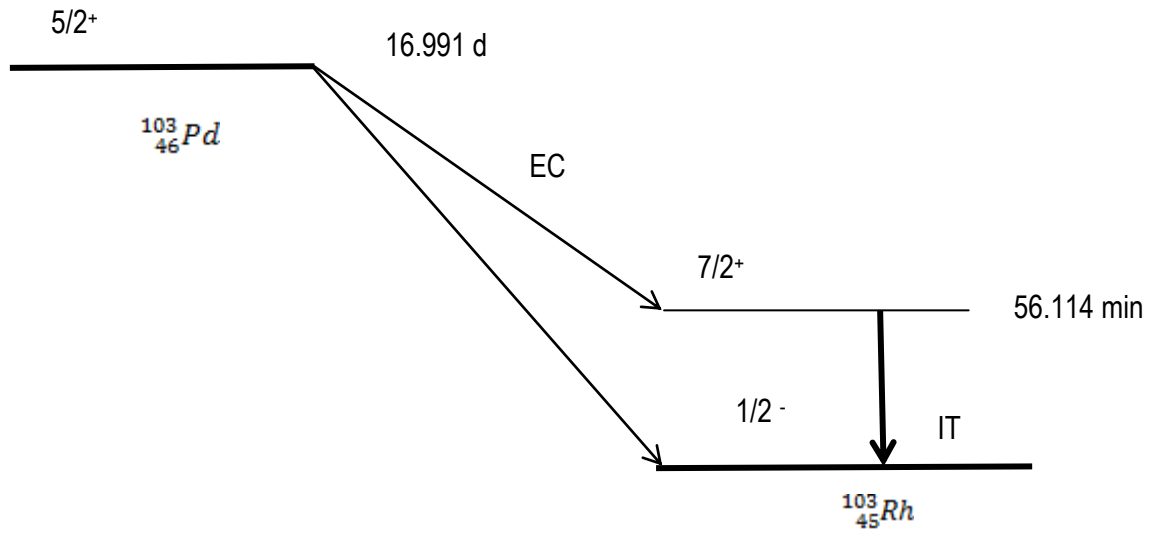

Figure 2: Simplified decay scheme of ^{103}Pd [25].

^{109}Cd has a half-life of 462.6 days, it decays to electron capture (EC) 100% by ^{109m}Ag [36-42] with the emission of γ-rays with energy of 88.03 keV (low quantum of 3.79%) along with the characteristic X-ray from K level, with energy of 22.54 keV (102%) [43-49]. ^{109}Cd of high X-ray abundance (99.83%) is excellent as a calibration source because the ^{109m}Ag daughter emits a single, low-energy γ-ray, and has a long enough half-life to ensure that it will be useful for a period of years [50].

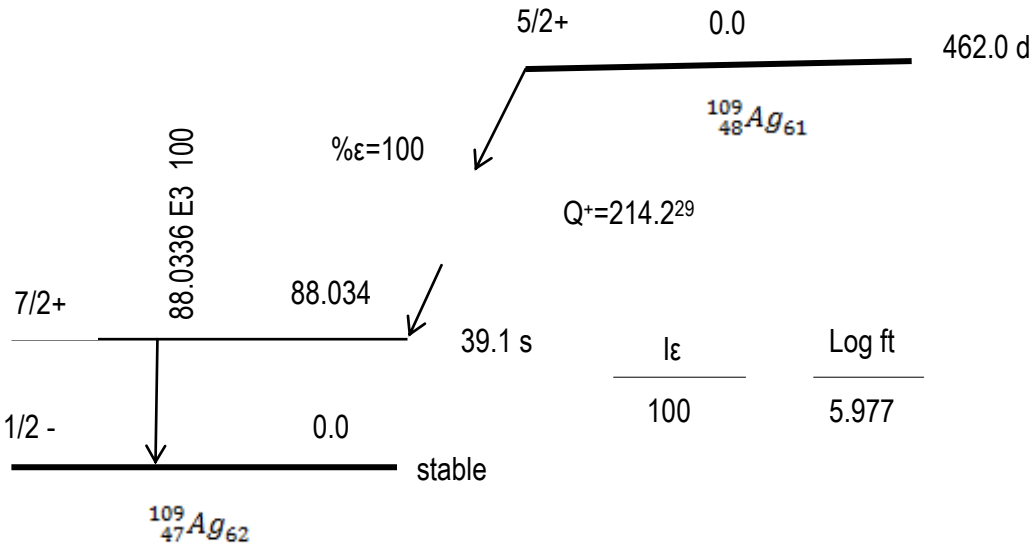

Figure 3: The ^{109}Cd and ^{109m}Ag decay scheme [51] (The level energies are in MeV).

1.2.2 Production of Radionuclides

Radionuclide production involves altering the number of protons and/or neutrons in the nucleus (target). If a neutron is added without the emission of particles, then the resulting nuclide will have the same chemical properties as those of the target nuclide. However, if the target nucleus is bombarded by a charged particle, a proton for example, the resulting nucleus will usually be that of a different element. The exact type of nuclear reaction a target undergoes depends on a number of parameters, including the type and energy of the

bombarding particle. Currently more than 80% of the medical radionuclides are produced by research reactors, the remaining radionuclides are made by particle accelerators such as circular accelerators (cyclotrons) and linear accelerators (linacs).

Cyclotrons come from a bigger family of electrical machines called accelerators, because they make particles to gain kinetic energy by applying electrical and magnetic fields to the particle trajectory so it can absorb energy from the media where it is travelling. Cyclotrons are the most commonly used devices for acceleration of particles to energies sufficient to bring about the required nuclear reactions. In a cyclotron, charged particles (S) such as protons, deuterons, α-particles, ^{3}He-particles and so forth are accelerated in circular paths within the dees (A and B) under vacuum by means of an electromagnetic field. These accelerated particles can possess a few kiloelectron volts (keV) to several billion electron volts (BeV) of kinetic energy depending on the design of the cyclotron [10]. The production of radionuclides with an accelerator demands that particle beams be delivered with two specific characteristics- (i) the beam must have sufficient energy to bring about the required nuclear reactions, and (ii) there must be sufficient beam current to give practical yields [52]. One clear advantage that accelerators possess is that, in general, the target and product are different chemical elements. This makes it possible to: (a) find a suitable chemical or physical means for the separation; (b) obtain high specific activity (SA) preparations, owing to the target and product being different elements; (c) produce fewer radionuclidic impurities by selecting the target material, particle and energy window for irradiation [36].

1.2.3 Nuclear Reaction of ^{103}Pd Production

For the production of ^{103}Pd, neutron, photon and charged particle induced reactions have been attempted and evidently, both reactors and cyclotrons are utilized for the production

purposes. However, cyclotrons appear to have a higher potential since both X-ray and Auger electron emitters are generally neutron deficient. Originally, ^{103}Pd can be produced by irradiation of palladium (Pd) with neutron in the reaction, which is based on natural palladium target containing 1.02% of ^{102}Pd. However, due to a low content of ^{102}Pd, the specific radioactivity achieved is rather low and this technique does not yield short-lived ^{103}Pd sufficiently for medical use [24,30,54]. A further possible disadvantage resides in the fact that large amounts of stable ^{102}Pd remain which may shield the low energy X-ray released when ^{103}Pd nuclei disintegrate [35].

Low isotopic abundance of ^{102}Pd in the natural mixture of palladium isotopes (1.02%) governs the usage of palladium highly enriched with this radionuclide as a target material. Unfortunately, the enrichment of palladium with ^{102}Pd rarely exceeds 50-80%, i.e. this material contains other palladium radionuclides, like ^{108}Pd and ^{110}Pd. These radionuclides produce other radionuclides during neutron irradiation. For example, ^{108}Pd produces ^{109}Pd ($T_{1/2}$ = 14 h) by (n,γ) reaction that difficult to separate from ^{103}Pd chemically. ^{110}Pd (n,γ), on the other hand, yields ^{111}Pd ($T_{1/2}$ = 23 min) that decays to ^{111m}Ag ($T_{1/2}$ = 7.5 d).Consequently, a radiochemical procedure should be applied to purify ^{103}Pd from radioactive silver impurity [32]. Other problems are associated with the above reference [55] and increasing the enrichment of ^{102}Pd leads to enhanced specific radioactivity of ^{103}Pd but still the product is used for internal therapy with caution. In contrast to reactor production of ^{103}Pd, its production from a cyclotron is very effective [24].

^{103}Pd can also be produced by different nuclear reaction such as:

1. The nuclear reaction ^{103}Rh(d,2n)^{103}Pd carried out in cyclotron with deuterons of approximately 20MeV energies. This reaction have a higher yield than (p,n) reaction but

since, in general, the deuteron beams available today at commercial cyclotrons are rather low, and the overall expected batch yield of ^{103}Pd would be quite small [56].

2. The nuclear reaction ^{106}Cd(n,α)^{103}Pd is carried out in a nuclear reactor . Irradiation of enriched cadmium-106 is also problematic since a high energy (40 to 50 MeV) cyclotron is required, with target yields limited due to a 250 μA beam current within the cyclotron. Furthermore, this method results in a low predicted marketable and high cost and low availability of ^{106}Cd [19].
3. ^{100}Ru(α,n)^{103}Pd, ^{100}Ru(α,2n)^{103}Pd [57], and ^{102}Ru(3He,2n)^{103}Pd [26,57] are achieved with a specific activity that is very low.
4. An alternate high energy accelerator route using the ^{nat}Ag(p,2pxn)^{103}Pd reaction has also been investigated at energy of 140 MeV [58].
5. ^{nat}Ag(p,x)^{103}Pd, this nuclear reaction is carried out in a medium-sized cyclotron with protons at energy range, 150-50 MeV approximately 70 MeV energy [23,59,60] , between 11 MeV - 80MeV energy [31] and at 60 MeV – 200 MeV energy [61].
6. ^{104}Pd(γ,n) [19,27], ^{nat}Pd(p,n) and ^{nat}Cd(p,n) [62]; *etc*.

Currently, the routine production of ^{103}Pd is done via the ^{103}Rh(p,n)^{103}Pd [29,56] reaction using a cyclotron with high intensity proton beams of energy typically < 20 MeV. However, at iThemba LABS the production of ^{103}Pd is done using the 66 MeV proton. The cross section for the process ^{nat}Ag(p,x)^{100,101,103}Pd are presented in Figure 4, 5 and 6 and it seems that the integral yield is high as shown in Figure 7 [31].

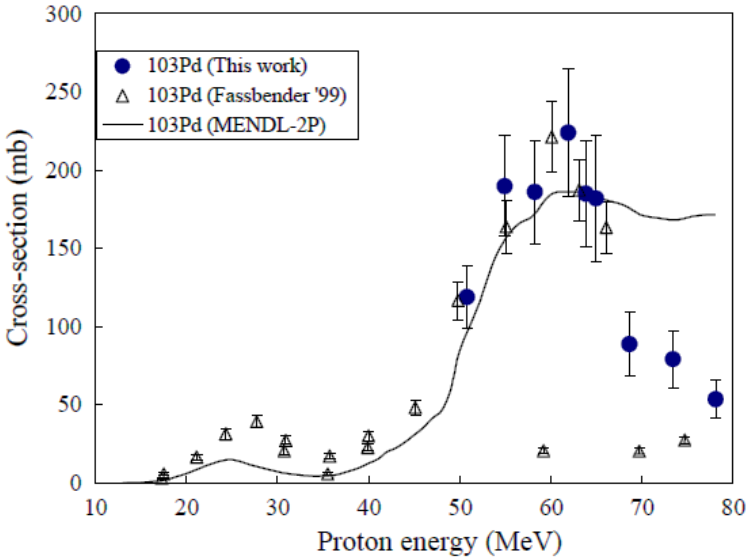

Figure 4: Excitation function of $^{nat}Ag(p,x)^{103}Pd$ reaction [31].

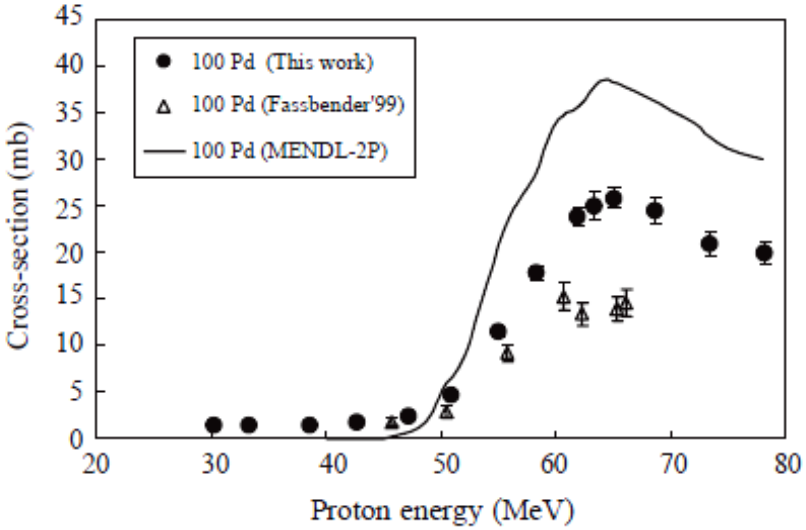

Figure 5: Excitation function of $^{nat}Ag(p,x)^{100}Pd$ reaction [31].

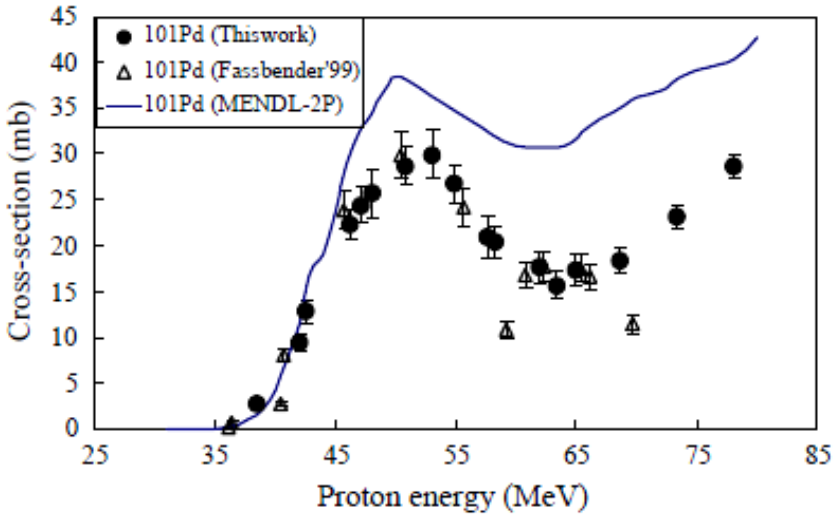

Figure 6: Excitation function of ^{nat}Ag(p,x)^{101}Pd reaction [31].

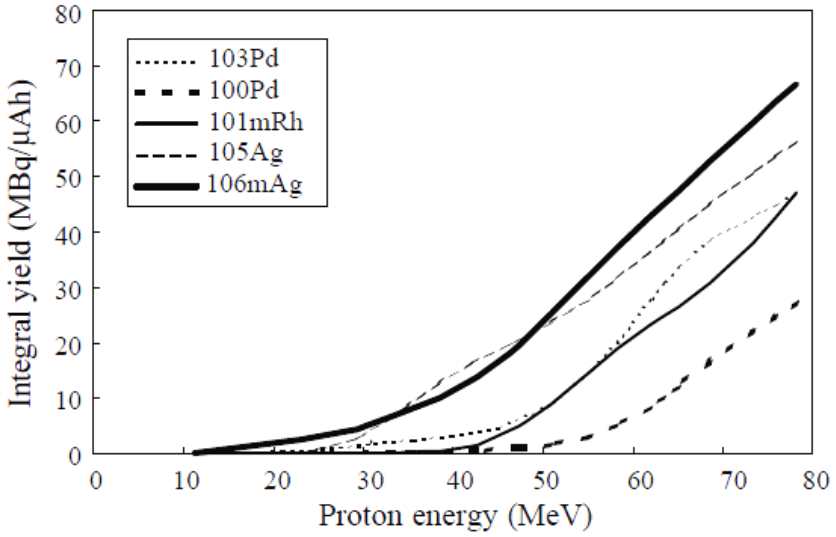

Figure 7: Integral yields as a function of proton energy for the production of ^{103}Pd, ^{100}Pd, ^{101m}Rh, ^{105}Ag and ^{106m}Ag radionuclides [31].

1.2.4 Nuclear Reaction of ^{109}Cd Production

Several routes for the production of ^{109}Cd have been reported in literature, namely proton, neutron and α bombardment of Ag, as well as proton bombardment of In [37,40,43,63,64]. Both reactors and cyclotrons are utilized for the production purposes. Many researchers have used silver as it is cheap and it requires less energy for the bombardment. Some nuclear reactions include the following:

a. ^{109}Cd may be obtained with the irradiation of targets with a high neutron flux at a nuclear reactor. In this case nuclear reactions ^{107}Ag (n, γ)^{108}Ag → ^{108}Cd (n, γ)^{109}Cd [63,64,65] and ^{108}Cd (n, γ)^{109}Cd and under irradiation of targets from enriched isotope of the ^{108}Cd are used [43,65];

b. The production of ^{109}Cd with deuterons beam (in cyclotron) can be performed by : irradiation of silver targets with deuterons on charged particle accelerators, i.e., reaction ^{109}Ag(d,2n)^{109}Cd [43,48], ^{nat}Ag(d,2n) with E_d= 13.4 MeV [43];

c. The production of ^{109}Cd with alpha particle induced silver target [67] ;

d. The production of ^{109}Cd with a proton beam can be performed by the following nuclear reactions:

   – Reaction channels include ^{nat}In(p, x)^{109}Cd (medium energy protons) [40], energy of about 96 MeV [44];
   – ^{109}Ag(p,n) reaction with 9 MeV [36,49];
   – ^{nat}Ag(p,n)^{109}Cd (E_p=15 MeV) [44,47], energy between 9 and 14 MeV [37,38,39]; with 36 MeV energy [45].
   – ^{nat}Cd+p with energy more than 80 MeV [68];
   – ^{115}In(p, 2p5n)^{109}Cd [69] and with enriched ^{109}Ag targets [70];

e. Pd+α with energy about 40 MeV [64], ^{nat}Pd(α, xn) [67] and ^{107}Ag(α,x) [36].

^{109}Cd is currently produced via proton irradiation of electroplated silver on a gold-coated copper backing [47] with the recovery of 88% without silver impurities.

The cross section for the process ^{nat}Ag(p,x)^{109}Cd is presented in Figure 8 where it shows that the better energy for the production of ^{109}Cd using ^{nat}Ag target was between 5 MeV and 15 MeV [39].

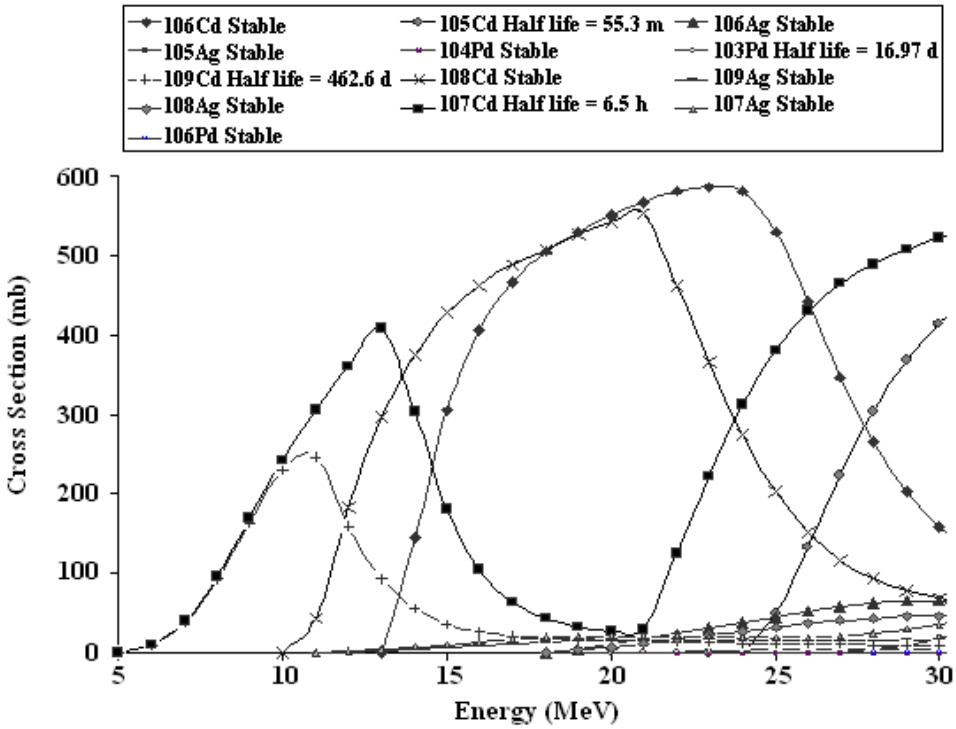

Figure 8: Excitation function of the ^{nat}Ag(p,x) for ^{109}Cd production using Alice code; ^{107}Cd (6.5 h), ^{106}Cd (stable) and ^{108}Cd (stable) impurities will be produce in energy range of 5 to 15 MeV [41].

1.3 APPLICATIONS OF RADIONUCLIDES

Radionuclides have very useful properties; radioactive emissions are easily detected and can be tracked until they disappear leaving no trace. These properties lead to many applications for radionuclides in the scientific, medical, forensic and industrial fields [2,71,72,73,74,75]. In

nuclear medicine, different goals are visualization of organs, localisation of tumours, detection of abnormalities in *diagnosis* (imaging), determination of metabolic pathways, introduction of radiation sources into specific sites for *therapy* [2,14,74,76,77]. In imaging, we have two main applications of radiotracers: Gamma imaging with usage of radionuclides such as ^{81m}Kr, ^{99m}Tc, ^{133}Xe, ^{67}Ga, ^{82}Rb, ^{201}Tl [74] and Photon Emission Tomography (PET) with usage of radionuclides such as ^{11}C, ^{13}N, ^{15}O, ^{18}F [78]. We also have others like ^{109}Cd for cancer detection, pediatric imaging, heart disease diagnostics [75] while in therapy, there are three general classes such as *brachytherapy*, *teletherapy* and *radionuclide therapy*. Examples of some radionuclides used in the treatment of different cancers: ^{47}Sc, ^{103}Pd, ^{159}Gd, ^{105}Rh, ^{90}Y, ^{64}Cu, ^{166}Ho, ^{211}At, ^{111}Ag, ^{77}Br, etc [2,75,78].

Radionuclides and radiation from X-ray machines and other devices have found widespread use in industrial and research. There are four major categories of applications of radionuclides and radiation in industry: radioisotope tracers (radiation traces materials), materials affect radiation (radiography and gauging), radiation affects materials (radiation processing) and radiation uses energy (nuclear batteries) [2,72,74,80]. Selected examples of radionuclides used on an industrial scale are: ^{109}Cd, ^{137}Cs, ^{131}I, ^{63}Ni, ^{90}Sr, ^{147}Pm, ^{3}H, ^{192}Ir, ^{252}Cf, ^{244}Cm, ^{230}Th, ^{210}Po, ^{235}U, etc [75]. After the irradiation of the target using the cyclotron, the target itself and the product are still mixed and must be separated in order to get the pure product to be used in medicine or industry. There are different methods for the separation of the product from the target like precipitation, extraction chromatography, rapid radiochemical separations, ion exchange, solvent extraction and so on [75].

For this work, ion exchange chromatography was chosen because it is easy to use in a hot cell environment and the removal of impurities in the separation process before eluting the radionuclide of choice, provides a much purer product than any other method used.

1.4 APPLICATIONS AND ADVANTAGES OF ION EXCHANGE CHROMATOGRAPHY AND ION EXCHANGERS

1.4.1 Ion Exchange Chromatography and Ion Exchangers

Ion exchange chromatography (IEC) involves sequential exchange and elution of ions from a column. Retention is based on attraction between solute ions and charge boundary on the stationary phase. The use of IEC was first reported by Taylor and Urey in 1938 to separate lithium and potassium isotopes using Zeolite resins, and by Samuelson in 1939 who demonstrate the potential of synthetic resins as a separation medium [79]. Although synthetic ion exchangers were known since 1935, the separation of the lanthanide fission products during the Second World War gave a powerful impetus to ion exchange chromatography. Ion exchange chromatography is classified into two major groups, namely, (a) cation exchange chromatography and (b) anion exchange chromatography. Ion exchange chromatography can be used in water treatment, sugar industry, food industry, chemical industry, pharmaceutical industry and so on. The advantages are that IEC is a non-denaturing technique which can be used at all stages and scales of purification, it can be controlled by changing the pH, salt concentration and/or the ion exchange media, it offers high selectivity and can serve as a concentrating step.

1.4.2 Types, Applications and Advantages of Ion Exchangers

Many different natural and synthetic products show ion exchange properties. The most important of these are ion exchange resins, ion exchange coals, mineral ion exchangers, and synthetic inorganic ion exchangers. Several other types of ion exchangers are historically interesting, but are now obsolete. Others are still used for special purposes. The general

structural principle framework is electric surplus charge and mobile counter ions, common to all ion exchangers.

1.4.2.1 Ion exchangers

Ion exchangers have many appearances: natural and artificial; inorganic (crystalline) and polymeric (organic). According to various authors and different applications, ion exchange materials have been classified into various ways, however, there are two general categories of ion exchange materials which are *inorganic (mineral-based) ion exchangers* and *organic ion exchangers* [81,82,83]. Considering the separation mechanism, ion exchangers can be further classified into various categories including ion exchange resins, chelating adsorbents, hydrogels, affinity polymers, and ion exchange membranes. Most of the ion exchange materials that are used (and have the potential to be used) in radiochemical process applications are synthetic materials. One of the reasons for the preferential use of synthetic materials is the relative ease with which the characteristics of the exchangers can be controlled by appropriate changes in composition and preparative methods, which are composed by the matrix (which is constitute by different monomers) and different functional groups.

Synthetic organic ion exchangers (organic or polymeric) are classified on the basis of (1) exchangeable species as cation, anion, ampholyte and multi-functional types; (2) functional groups as strong, weak, acid/base types; (3) preparation as polymerization types and condensation types and (4) rigidity of polymeric structure as microporous (gel) and macroporous (macroreticular and isoporous) types.

Table 1: Properties of Ion Exchange Resins [79].

Chemical	**Physical**
Type of the matrix	Physical structure and morphology
Cross-linking degree	Particle size
Type of functional groups	Pore size and morphology
Ion exchange capacity	Surface area
Ionic form	Partial volume in swollen state

In this work, for the separation of radionuclides, ion exchange resins (polymeric resins) as anion exchange resins and chelating resins will be used. The choice of ion exchange resins used during the separation of radionuclides produced (^{103}Pd and ^{109}Cd) from the tandem ^{nat}Ag/^{nat}Ag targets was done based on the distribution coefficients of the radionuclides to be separated.

1.4.2.2 Anion exchange resins and Chelating resins

The synthetic organic resins consist of a three dimensional cross-linked polymer matrix (network, skeleton) which is functionalized to provide their ion exchange capacity (formation of a solution in contact with the solvent) and hinders the motion of the polymer chains. The matrix undergoes additional reactions to provide the strong acid cation, strong base anion (type I and type II), weak acid cation or weak base anion functionality. Besides different main chains, the diversity of three-dimensional structures is also provided by the use of different cross-linking agents. The most commonly used materials as the matrix for ion exchange are polymers based on the copolymerization of styrene cross-linked with

divinybenzene which is prepared by pearl polymerization. The degree of cross-linking or the density of cross-links between polymeric chains [79] influences the structure of the matrix, its elasticity, swelling ability of the material, and mobility of the counter ions inside the exchanger, among others. Conventionally, the cross-linking degree is expressed as percentage of the cross-linking reagent introduced in a reaction mixture at the synthesis stage. For example, a well-known ion exchange resin Dowex 50X8 (produced by Dow Chemical for several decades) contains 8% of divinylbenzene molecules.

The table 2 below indicates different types of functional groups of ion exchange.

Table 2: Functional groups of ion exchangers

Cation exchangers		**Anion exchangers**	
Type	Functional group	Type	Functional group
Sulfonic acid	$-SO_3^-H^+$	Quaternary amine	$-N(CH_3)_3^+OH^-$
Carboxylic acid	$-COO^-H^+$	Quaternary amine	$-N(CH_3)_2(EtOH)^+$
Phosphonic acid	$PO_3^-H^+$	Tertiary amine	$NH(CH_3)_2^+OH^-$
Phosphinic acid	$HPO_2^-H^+$	Secondary amine	$-NH_2(CH_3)_2^+OH^-$
Phenolic	$-O^-H^+$	Primary amine	$-NH_3^+OH^-$
Arsonic	$-HAsO_3^-H^+$		
selenonic	$-SeO_3^-H^+$		

a. Anion Exchangers

The first commercial anion exchange resins, Wofatit M, were of weakly basic character and were obtained by the condensation of *m*-phenylenediamine and polyethylene-imine with formaldehyde. Anion exchange resins are subdivided into two categories: styrenic anion exchange resins and acrylic exchange resins. In these categories, we can have strong basic anion exchangers, mild basic anion exchangers and weak basic exchangers.

Background of the AG1-X10 resin

AG 1-X10 resin is a strongly basic anion exchanger manufactured by Bio-Rad Laboratories and is supplied in a chloride form. It exchanges anions of acidic, basic and neutral salts, and ampholytes on the basic side of their pH. AG 1-X10 resin is strongly basic anion exchanger with quaternary ammonium functional groups attached to the styrene divinylbenzene copolymer lattice. The cross-link degree of the resin is 10 %.

b. Chelating Exchangers

Some resins have been developed with functional groups specifically to adsorb certain types of ions having the status of metal-ion-specific exchange resins known as chelating ion exchangers or chelating ion exchange resins also known as specific exchangers or chelating sorbents are a subgroup of ion exchange resins. The selectivity of these resins depends more on the complex that is formed than on the size or charge of the ions; this development was owing to the lack of selectivity, sensitivity, and capacity of the conventional ion exchange resins particularly for trace heavy metal ions [81,82]. A high selectivity of chelating ion

exchangers lies in their ability to form stable, often covalent, complexes of varying strength with metal ions.

Background of the Chelex-100 resin

Chelex-100 is a chelating ion exchange resin manufactured by Bio-Rad Laboratories. Analytical grade Chelex-100 chelating resin is composed of styrene divinylbenzene copolymers with iminoacetate functional groups. Iminoacetate ions act as chelator which chelates polyvalent metal ions. This resin is very useful in binding metal contaminants with a high selectivity for divalent ions, without altering the concentration on non-metal ions. Chelex-100 is classified as a weakly acidic cation exchange resins by virtue of its carboxylic acid groups, but it differs from ordinary exchangers due to its high selectivity for metals ions (divalent) and its much high bond strength. At low pH, Chelex-100 acts as an anion exchanger due to their imines, nitrogen and carboxyl groups which are protonated, and, the protonated nitrogen becomes positively charged and can attract anions while carboxyl groups are neutral and unreactive. As pH increases, anion sorption decreases and the cation sorption start to increase until pH>12 and in this case the resin functions solely as a cation exchanger.

1.4.3 Radiochemical separations of ^{103}Pd and ^{109}Cd

1.4.3.1 Radiochemical separation of ^{103}Pd from silver target

^{103}Pd prepared from silver targets can be purified using different ways. Faβbender *et al*. [59] used two different ion exchange resins. At the outset, the target was dissolved in 2 mL concentrated HNO_3, 500 μL $Pd(NO_3)_2$ solution as a carrier was added to the solution and diluted with water. The separation of ^{103}Pd from Ag and Rh was performed into two steps. In

the first step, Pd and Rh were separated from Ag, using the chelating Chelex-100 resin (equilibrated with 0.5 M HNO_3) and the elution of Pd was done with 10 M HCl. In the second step, Pd was separated from traces of Rh on an AG 50W-X4 cation exchange resin using thiourea-HCl media, the column was rinsed with water and Pd was eluted with 4 M HCl. The disadvantage of this process was that it was a time consuming two-column process with numerous additional operations to remove the thiourea from the final product which ultimately gave low production yiel0d due to losses at various stages of the chemical processing.

Mausner *et al*. [58] employed two Chelex 100 resin columns with different sizes respectively. The dissolved target was evaporated to dryness, re-dissolved in 0.4 M HNO_3 and passed over a 10 mL Chelex-100 resin column (column 1). The column was then washed with 1 M HNO_3 to elute the remaining Ag, as well as Tc, Rh, and Ru radionuclides. The Pd (with traces of Ag and Rh) was stripped from the column with 10 M HCl. This solution was evaporated to dryness, re-dissolved in 0.4 M HNO_3, and passed over another smaller Chelex-100 resin column (column 2). The column was washed with 1 M HNO_3, the Pd was again eluted with 10 M HCl. The final product was ~ 99% pure with some Rh impurities.

Aardaneh *et al.* [60] used a single step AG MP-1 anion exchange resin column for the separation of Pd radionuclides from Rh and the Ag target and the average recovery of ^{103}Pd was 97%. After dissolving the target, the re-dissolved solution containing Pd carrier was loaded onto the column pre-equilibrated with 3 M HNO_3. For the elution of Rh and Ag, 3 M HNO_3 solution was used and 5% ammonia solution was used to elute the Pd. The average recovery of Pd was 97.4%, however; the shortcoming of this process was the evidence of the impurity of ^{100}Pd in the final product of ^{103}Pd and for a routine production of ^{103}Pd from an

Ag target by high energy cyclotron, although by losing more than a half of the original activity, it is advisable to do the radiochemistry at least 20 days after the bombardment [60]. Besides ion exchange techniques, Lapashina et al. [61] employed a precipitation system for the separation of ^{103}Pd from the major part of the Ag target and followed this with further purification of Pd from other nuclides (Rh, Ru and Tc) using the sorption of chelating exchanger such as Polyorgs-15 and Polyorgs-32. The disadvantages of this method was during the filtering process the precipitation of silver chloride, the use of palladium stripping with hot hydrochloric acid, resulting in the failure of the hot cell equipment, insufficient removal of impurities (Ag and Rh), and the difficulty of performing certain stages of the process.

1.4.3.2 Radiochemical Separation of ^{109}Cd from silver target

Most researchers with the exception of Aardaneh *et al.* have used silver electroplated on copper during the ^{109}Cd production [45]. In a simultaneous production of ^{57}Co and ^{109}Cd using a cyclotron by Landini and Osso [39], Ag (~0.4 g) was dissolved in 20 mL of concentrated HNO_3 and the solution evaporated to dryness and then dissolved with 20 mL of H_2O. The evaporation to dryness was repeated until the solution reached pH between 2 and 7. About 1.25 g of eletrolitic Cu were added and the solution was stirred for 15 minutes to reduce Ag^+ to Ag^0. The reduced Ag and the excess of Cu were filtered by quantitative filter paper and the filtrate containing ^{109}Cd, Cu^+ and traces of Ag^+, was heated to dryness and further dissolved with 8 M HCl. This last step was repeated twice. The final solution (10 mL in 8 N HCl) was percolated into an anion exchange resin Dowex 1X8 (50–100 mesh, 7 cm high x 1 cm diameter), previously conditioned with 8 M HCl. Under these conditions, ^{109}Cd was adsorbed on the resin leaving Cu^+ and Ag^+ free in the solution. These radionuclides were later eluted with 0.1 M HCl with a recovery of ~80%.

In 2007, Aardaneh *et al.* [45] used concentrated HNO_3 to dissolve the Ag target and the solution was evaporated to dryness and then dissolved with H_2O. The evaporation was repeated until the aqueous solution reached a pH between 2 and 7. They added metallic Cu turnings to the solution and stirred for 30 minutes. Cu was used in order to reduce Ag^+ to Ag^0 $Cu\,(s) + 2Ag^+(aq) \rightarrow Cu^{2+}(aq) + 2Ag\,(s)$. The reduced Ag and the excess Cu were filtered off on a filter paper in a syringe, supported by glass fiber at the bottom. 30% H_2O_2 was added to the filtrate, evaporated to dryness and the residue was dissolved with a mixture of 2 M HCl and 30% H_2O_2. The filtrate containing ^{109}Cd, trace amount of Ag radionuclides and substantial amounts of Cu^{2+} ions was loaded to the column (4 cm×1.6 cm^2) packed with the AG1-X10 anion exchange resin and pre-conditioned with 50 mL 2 M HCl at a flow rate of 2 mL/min using a peristaltic pump. The column was washed with 200 mL of 2 M HCl containing 5 mL H_2O_2 to remove any Ag traces as well as Cu^{2+} and Cu^+. For the elution of ^{109}Cd, 50 mL 1 M HNO_3 was used and the yield was 96%.

Gholamzadeh *et al.* [47] reported that the irradiated natural silver-electroplated target on the gold layer was dissolved efficiently with liquid flow-through stripper acidic system of 14 M HNO_3 and the dissolved target was evaporated using a condenser system at 180 °C and the recovered solution was examined for Ag impurities. During this work, the authors separated ^{109}Cd from the silver target using evaporation at 180 °C. The dissolved target was heated by a heater/ stirrer at 180 °C and after a condenser system was used to guide cadmium nitrate steam to an Erlenmeyer flask and allowed to cool. These authors took advantage of the difference in boiling points of cadmium nitrate and silver nitrate, which are 132 °C and 444 °C, respectively [47].

A precipitation method was used by Maiti *et al.* (2011) to separate ^{107,109}Cd from a proton induced silver target [84]. The target was dissolved with 0.1 M HNO_3 and Ag was precipitated with 0.1 M HCl and this step was repeated. The final radiochemical yield of ^{107,109}Cd was greater than 99.8 %.

1.5 PROBLEM STATEMENT

The use of radionuclides such as ^{103}Pd as a permanent interstitial seed for the treatment of prostate cancer and other tumours and the application of ^{109}Cd for the inhibition of liver cancerous cell have attracted considerable interest during the last decade. However, the quality and quantity of supplies of ^{103}Pd and ^{109}Cd remains a challenge. The production of ^{103}Pd is mostly accomplished by a cyclotron proton beam on a rhodium plated target or by enriched ^{102}Pd in the reactor. However, ^{102}Pd is contaminated with ^{108}Pd and ^{110}Pd which produce ^{111}Pd. These radionuclides are difficult to separate and this makes the product not suitable for use in the treatment of cancers due to high γ-rays radiations. For Rh, on the other hand, the dissolution of the target is so hard due to extremely low reactivity of Rh metal in acidic and alkaline media. The recycling of radioactive Rh target material after the separation is very complex. The cost for the enriched ^{102}Pd or ^{103}Rh is high. In 2009, the price of ^{103}Pd seed sources was approximately 10 US dollar for 1 mCi while one run of brachytherapy consumes about 50 to 70 mCi [54]. All these problems stated above make the ^{103}Pd product not affordable by everyone who needs it for its therapy. The numbers of prostate cancer, breast cancer and eye tumor patients, on the other hand, continue to increase worldwide.

Currently, ^{109}Cd is produced via natural silver electroplated to copper, however, the chemical separation of ^{109}Cd from the target remains complicated and long. Moreover, the use of ^{109}Cd

in industry for determining the metallic composition of samples or analyze metallic alloys and check stock and sort scrap and particularly in medicine is still growing fast.

1.6 AIMS AND OBJECTIVES

The increase in demand of ^{103}Pd for permanent interstitial implants for different cancers and that of ^{109}Cd as a source of radiation for X-ray fluorescence analysis and as a ^{109}Cd/^{109m}Ag generator and examining their price (^{103}Pd and ^{109}Cd) over the world prompted us to investigate alternative methods for their production and separation. This led to the following objectives:

- To produce ^{103}Pd and ^{109}Cd using a tandem natural silver target (Ag/Ag) bombarded with a 66 MeV proton beam from a cyclotron.
- To determine an optimal method for the radiochemical separation of ^{103}Pd and ^{109}Cd using ion exchange chromatography.

CHAPTER 2: RESULTS AND DISCUSSION

2.1 TARGETRY

In the previous investigations, the irradiation of the target (^{nat}Ag) to produce ^{103}Pd and ^{109}Cd was done separately using the single 66 MeV proton beam of the Separated Sector Cyclotron [45,59]. Lately, this procedure proved to be less attractive because as the market demand for pure ^{103}Pd and ^{109}Cd continue to increase and additional proton beam time is required to meet the production demand. Constraints of the expensive proton beam of the cyclotron to produce these radionuclides were becoming a limiting factor. Instead of using the separate 66 MeV proton beam for the irradiation of each Ag target to produce the ^{103}Pd and ^{109}Cd separately, it was postulated that a single 66 MeV proton beam could be used to irradiate a tandem ^{nat}Ag/^{nat}Ag target because the optimal energy range required to produce ^{103}Pd and ^{109}Cd ranged between 70-40 MeV and 30-10 MeV, respectively [31,36,41,59]. According to the cross section calculated by Faβbender et al. [59] and Uddin et al. [31] (see Figures 4, 5 and 6, Section 1.2.3), it seems that using natural silver target with a high energy cyclotron (60 – 70 MeV), and in particular in iThemba LABS case where the 66 MeV proton is used, can be profitable for ^{103}Pd production. With the investigations on the production yields of the radionuclides produced in the ^{nat}Ag(p,n) nuclear reactions, i.e., ^{109}Cd, ^{107}Cd ($T_{1/2}$ = 6.5 h) and ^{106m}Ag ($T_{1/2}$ = 8.46 d), Landini et al. [38] suggested that the optimum energy range for the production of ^{109}Cd is 14–9 MeV as in this energy range the contamination of ^{106m}Ag is minimized. Mirzaii et al. [41] used an energy of 9 MeV, however, the production yield decreased considerably. The authors recommended a 35 mm thickness of the silver for 15 MeV entrance of the proton beam with a 5 MeV exit (see Figure 8, Section 1.2.4) because the silver targets easily withstand a high proton beam [41]. Thus, silver target could be irradiated by low-medium energy accelerators even for a long time for ^{109}Cd production.

In this work, we bombarded a tandem $^{nat}Ag/^{nat}Ag$ target simultaneously using the same single 66 MeV proton beam to produce ^{103}Pd and ^{109}Cd. The ^{103}Pd was produced in the high energy slot (62.515 MeV- 40.173 MeV) whilst ^{109}Cd was produced in the low energy slot (38.652 MeV- 0 MeV). This tandem Ag/Ag arrangement shown in Figure 9 and Table 3 has made it possible to increase the production yields of both ^{103}Pd and ^{109}Cd two fold by using the same beam time that was available for the separate irradiations.

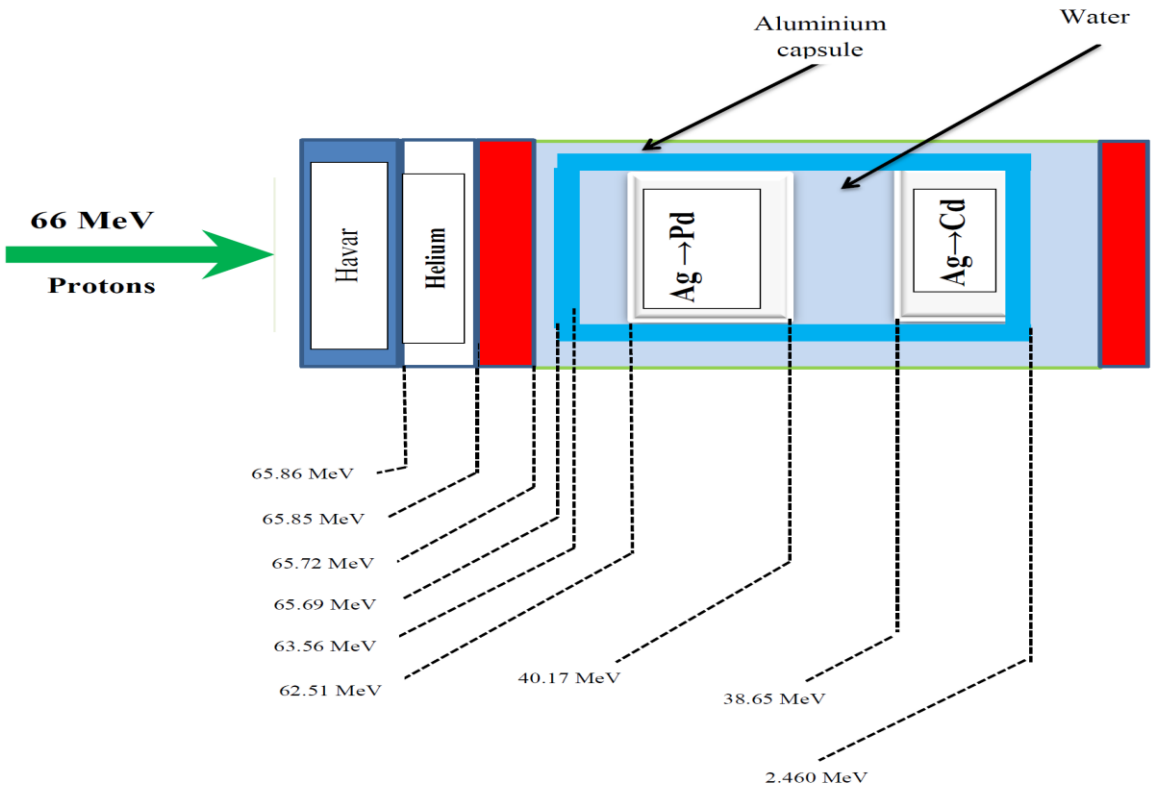

Figure 9: Beam Degradation Profile of Ag/Ag target

Table 3: Target Energy Degradation

Layer	Thickness (mm)	Energy In (MeV)	Energy Out (MeV)	Energy loss (MeV)
Havar	0.025	66.00	65.86	0.139
Helium	10.00	65.86	65.85	0.002
Havar	0.025	65.85	65.72	0.139
Air	18.00	65.72	65.69	0.021
Aluminum	1.00	65.69	63.56	2.137
Water	1.00	63.56	62.51	1.047
Silver	**3.00**	**62.51**	**40.17**	**22.34**
Water	1.00	40.17	38.65	1.521
Silver	**3.00**	**38.65**	**Stopped at 2.460**	

2.2 RADIOCHEMICAL SEPARATION OF ^{103}Pd AND ^{109}Cd

In this investigation, we opted for ion exchange chromatography to separate Pd and Cd from a large amount of Ag target material (irradiated ^{nat}Ag targets). The choice was influenced by the simplicity of manipulation in a hot cell environment to provide a much purer product than the other methods. Two prominent procedures for the radiochemical separation of ^{103}Pd from Ag targets have been described in the literature by Faβbender *et al.* [59] and Mausner *et al.* [58] For the preliminary work, a previously developed method used at iThemba LABS [59] for the separation of ^{103}Pd from an irradiated Ag target which used two resin columns (Chelex 100 chelating resin and AG 50 W-X8 cation exchange resin) and also the procedure of Mausner *et al.* [58] (10 mL Chelex 100 chelating and 4 mL Chelex-100 chelating resins) were adapted to

this work. In the work of Dardenne et al. [85], it was shown that using the chelating resin Chelex 100 resin, the distribution coefficient of the Ag^+ ion as a function of nitric acid concentration (1 - 6 M) showed a low sorption of Ag^+ as $Ag(NO_3)_2^-$. The Ag was easily eluted from the chelating resin with 1 M HNO_3. In the work of Samczynski et al. [86] and Ceo et al. [87] it was shown using this chelating resin that in the 0.1 - 1 M HCl range, the anion exchange function of the Chelex-100 resin starts to be active due to protonation of the iminodiacetic groups and Pd, Ag and Rh exhibited a high absorption on the resin. The Pd, Ag and Rh could only be eluted from the Chelex 100 resin using concentrated HCl.

We investigated the conditions for the optimal purification of Pd from Ag and Rh using the varying size of Chelex-100 resin columns and using 1 M HNO_3 for the elution of Ag and Rh and 10 M HCl for the elution of Pd following the above literature precedents. The radiochemical separation of ^{103}Pd from ^{nat}Ag was achieved with the use of by using a single chelating Chelex 100 resin column. We manipulated the column size and the quantity of the $Pd(NO_3)_2$ carrier solution added during the loading step to determine the optimal radiochemical separation conditions. For the preliminary work as described in 4.4.1 and in 4.4.2, the use of a Ag target in combination with prepared trace amounts of Pd, Rh and Ag radionuclides were found to be very useful in determining the optimal conditions for the chemical separation. The measurement of ^{103}Pd activity (low abundance of 0.02% at 357 keV) in the solution containing Pd, Rh and Ag radionuclides with a HPGE detector proved to be problematic as a result of the high activity of Ag (^{105m,106}Ag) and Rh (^{101}Rh) radionuclides that interfered with the ^{103}Pd. However, because other Pd radionuclides such as ^{100}Pd and ^{101}Pd were co-produced with ^{103}Pd, it was decided to use the ^{100}Pd (84 keV) when tracing this radionuclide during the chemical separations. To trace the Rh radionuclide, ^{101}Rh at 127 keV and 307 keV, and for the Ag radionuclide, ^{105}Ag at 280 keV and 345 keV were successfully used. The number of counts under each specific keV peak as determined by the

HPGe detector was used to determine the activities of each radionuclide. During the preliminary work, the chemical separation of the Ag target in combination with the trace amounts of Pd, Rh and Ag radionuclides on the various size Chelex resin columns had shown varying results as indicated in Table 4.

In the preliminary run 1, the 3 cm x 1 cm Chelex resin column which was equilibrated with 0.5 M HNO_3 only retained 70% of the Pd radionuclides on the Chelex resin column. However, when the Pd radionuclides were eluted from the resin column with 10 M HCl no traces of Rh or Ag radionuclides were detected in the final product. The 30% loss of Pd radionuclides during the loading step was however not acceptable. In preliminary run 2, when using a larger Chelex resin column of 16 cm x 1.5 cm, the retention of the Pd radionuclides on the resin column increased to 95%. However, trace amounts of Rh and Ag radionuclides were detected in the final product of the Pd when it was eluted with 10 M HCl. Due to the length of the column, a large volume of 10 M HCl was used to elute Pd from the resin. During both preliminary runs 1 and 2, the amount of $Pd(NO_3)_2$ added to the loading solution to aid retention of the Pd radionuclides on the resin column was only at 0.01 g. It was therefore decided to increase the $Pd(NO_3)_2$ for subsequent preliminary runs to see if the retention of Pd radionuclides could be improved.

In preliminary run 3, the 11 cm x 1 cm Chelex resin column was used under similar conditions employed for the preliminary runs 1 and 2. However, the amount of $Pd(NO_3)_2$ was increased (0,028 g) and the retention of Pd radionuclides was 96% with 4% of Rh in the final product as a contaminant. In preliminary run 4, the column size was increased to 13 cm x 1 cm with the same conditions as in preliminary run 3. The Pd radionuclides were retained at 99% and the amount of Rh radionuclide contaminant found in the final product was less than 1%. In subsequent preliminary runs 5 and 6, using the same conditions as in 4, but reducing

the amounts of the $Pd(NO_3)_2$ to 0.021 g and 0.012 g, respectively, had shown as expected a drop in the retention of Pd radionuclides to 93% (preliminary run 5) and 87% (preliminary run 6).

The accurate amount of $Pd(NO_3)_2$ added to the loading solution seem to play an important role in the chemical separation of Pd radionuclides from the Rh and Ag radionuclides (inclusive of the 9 g ^{nat}Ag target). The $Pd(NO_3)_2$ in an acid medium also provided a significant yellow band on the Chelex resin column that made it easy to track the Pd radionuclides during the chemical processing as shown Figure 10. The $Pd(NO_3)_2$ increases the retention of Pd on the resin and the final product will be $[^{103}Pd]Pd^{2+}$. The separation of ^{103}Pd from ^{nat}Ag target performed after 20 days from the end of bombardment (EDB) in analogy with the work by Faβbender et al. [59] resulted in only 0.47% of ^{100}Pd remaining in the target.

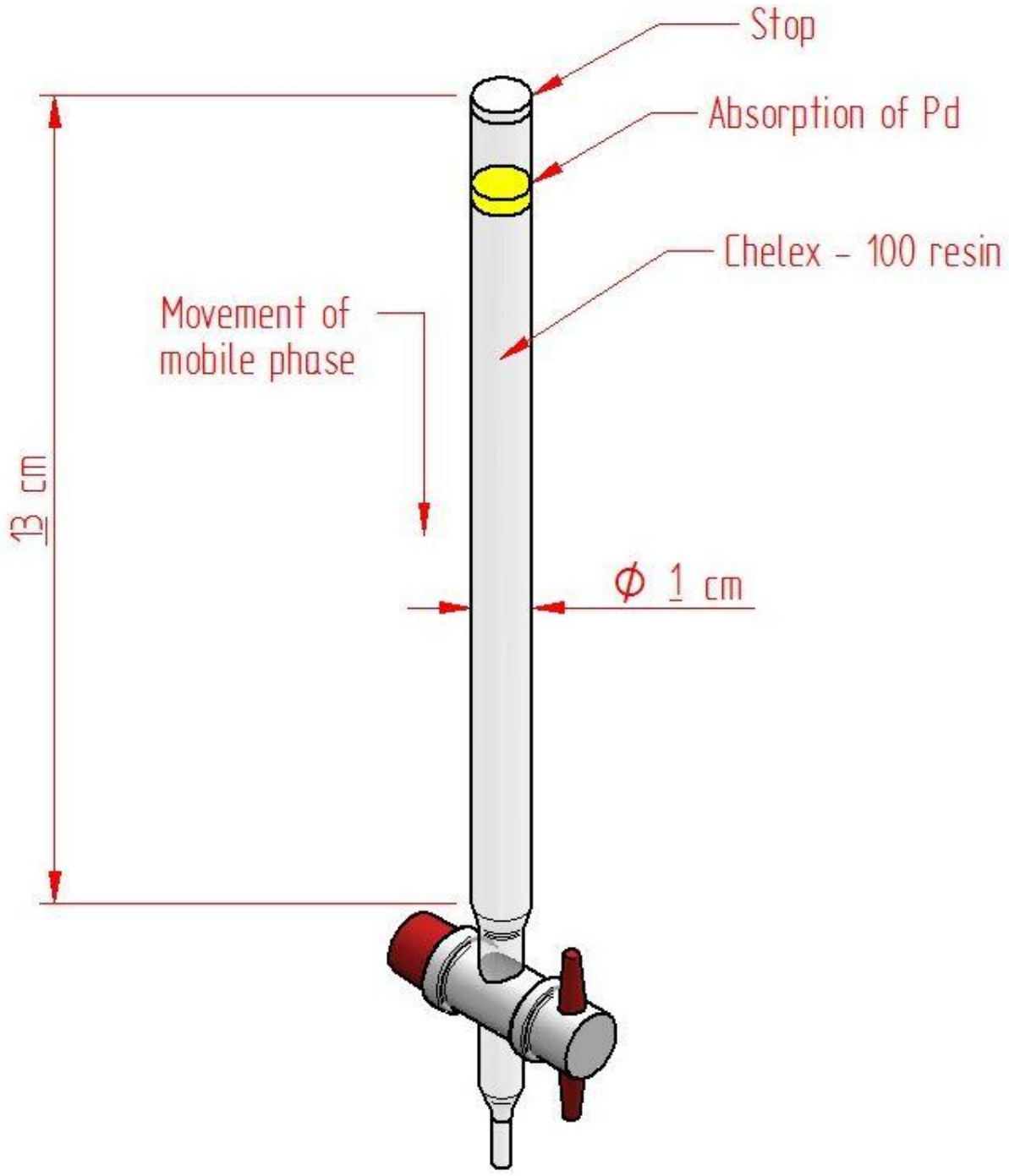

Figure 10: Chelex resin column with the yellow band

Table 4: Preliminary runs of Pd, Rh and Ag column chemical separations

Preliminary run	**Column size (cm)**	**$Pd(NO_3)_2$ (g)**	**Pd retained on the column during loading step (%)**	**Contaminant in the final product % Rh**	**Contaminant in the final product % Ag**
1	3 x 1	0.010	70.1	0	0
2	16 x 1.5	0.010	95.0	5.0	5.0
3	11 x 1	0.028	96.0	4.0	0
4	13 x 1	0.028	99.0	<1.0	0
5	13 x 1	0.021	93.0	0	0
6	13 x 1	0.012	87.0	0.8	0

Table 5 shows that with γ spectrometry it is difficult to detect the ^{103}Pd due to its abundance as discussed above. The presence of ^{103}Pd was confirmed by the amount of ^{100}Pd detected in solution.

Table 5: Radionuclide impurities of ^{103}Pd final solution using Chelex-100 / 1 M HNO_3 system

Nuclide	Half-life	Energy, KeV	Counts 3 m slit	
			Original	Final
^{100}Pd	3.63 d	84.0 (45 %)	239.0	235.0
^{101m}Rh	4.34 d	306.86 (93.5 %)	2210.0	39.0
^{105}Ag	41.29 d	344.52 (41.4 %)	2460.0	ND*
^{103}Pd	16.99 d	357.45 (0.02 %)	ND*	ND*

*ND: Not Detected

The elution curve (Figure 11) described the behavior of Pd, Ag and Rh on a Chelex-100 resin column (length 13 cm & inner diameter 1 cm) where the eluent, 1 M HNO_3 (335 mL) was used to elute the Ag and Rh from the resin column. 10 M HCL (100 mL) as an eluent was used to elute the Pd with no loss of Pd during the loading and washing steps.

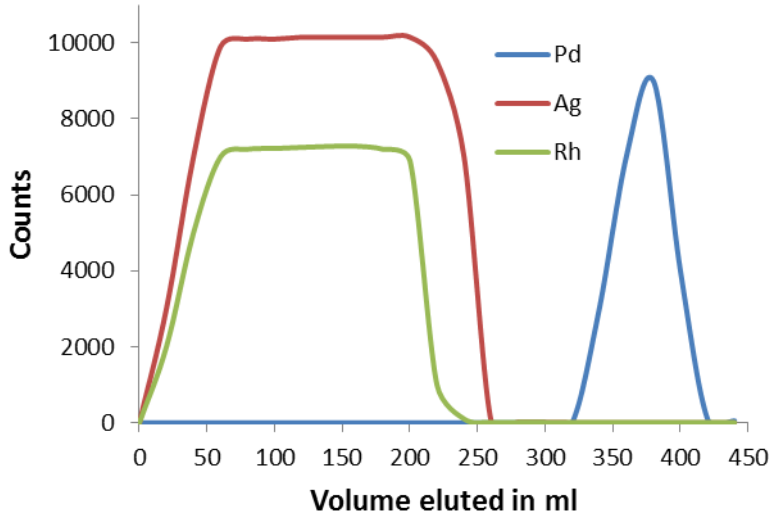

Figure 11: Elution curve for Pd, Ag and Rh on Chelex-100 resin column (length 13 cm & inner diameter 1 cm) with eluents 1 M HNO_3 (335 mL) for Ag and Rh and 10 M HCL (100 mL) for Pd.

For the hot cell runs, the irradiated Ag target that was located in the high energy window and that was processed with the same experimental conditions to that of preliminary run 4 [13 cm x 1 cm Chelex resin column with 0.028 g $Pd(NO_3)_2$] had shown consistent results as shown in Table 6. All 3 hot cell runs had shown a100% retention of the Pd radionuclides during the loading step and when the final product was eluted, no Ag radionuclides were found. The Rh radionuclides were found to be <1 % in the final product and this was consistent with preliminary run 4. The irradiation time of the Ag target for the 3 runs ranged between 10 and 60 mins and this gave a consistent production yield of ^{103}Pd at 1.5 mCi /µAh at end of bombardment (projected from data at the end of separation).

Table 6: Hot runs of Pd, Rh and Ag column chemical separations

Hot run number	Pd retained on the column (%)	Contaminant in the final product % Rh	Contaminant in the final product % Ag	Total irradiation time on target (mins)	^{103}Pd activity at end of the bombardment (mCi)
1	100.0	<1	0	10	3.87
2	100.0	<1	0	30	12.12
3	100.0	<1	0	60	24.30

Standard deviation: 3.87±0.05; 12.12±1.02; 24.34±0.06. Values are mean ± standard deviation (n=2). Means with different letters within same column are significantly different ($p<0.05$).

For the purification of ^{109}Cd, the procedure of Aardenah et al. [45] was adapted as a basis of this work, where the anion exchange AG1-X10 resin column was used to separate the ^{109}Cd from Ag and Rh. In the work of Kraus and Nelson [88] it was established that a table of distribution coefficients which showed the behavior of metal chloride complexes at trace ionic concentration in the presence of a strong base anion exchange resin. They have concluded that transition metals and noble metals can form anion chloride complexes with varying affinity for anion exchange resin. Thus, the sorption of Cd was relatively higher than that of Ag and Rh in 2 M HCl when using an anion exchange AG1-X10 resin. It was also shown by Saito et al. [89] and Faris et al. [90] that Cd, Ag and Rh cannot be absorbed on the AG1-X10 resin in 1 M HNO_3. Using the distribution coefficients of these different radionuclides [31,38,41,59], one was able to improve the efficiency of the chemical separation of ^{103}Pd and ^{109}Cd from tandem Ag/Ag targets material.

To track the chemical separation of Cd, Rh and Ag radionuclides, we used the following prominent energy peaks of each radionuclide: ^{109}Cd (88 keV, 3.92 % abundance), ^{105g}Ag (344.5 keV, 41.6% abundance) and ^{101m}Rh (306.9 keV, 86.3% abundance). In the first part of this work, the dissolution of the Ag target in concentrated HNO_3 and the reduction of Ag with Cu turnings (30 g) were easily accomplished and were found to perform at similar levels to the previous work [45]. However, in the second part of the work which involved the absorption of the Cd filtrate onto a AG1-X10 resin column and the elution of the Cd radionuclides from the column had shown far superior results when using a 6 cm x 1.5 cm resin column (preliminary run 4-6) compared to using a 4 cm x 1.6 cm resin column (previous work, preliminary run 1-2) and a 5 cm x1.6 cm resin column (preliminary run 3) as shown in Table 7.

In preliminary runs 1-3, the radionuclide impurities of Ag and Rh were found in the final product of the ^{109}Cd, but using the longer resin column resulted in a high purity ^{109}Cd with no Ag or Rh radionuclides detected in the final product. This was largely attributed to the longer resin column that was used as well as ensuring that the appropriate amount of Cu turnings was used to reduce all the silver to silver ion (Ag^+) in order to achieve an optimal chemical separation. As shown in Figure 12 this was confirmed by the elution curve of Cd, Ag and Rh on AG1-X10 resin column (length 6 cm & inner diameter 1.5 cm) where the eluent, 2 M HCl (365 mL) was effectively used to elute the Ag and Rh from the resin column and, the eluent 1 M HNO_3 (100 mL) was effectively used to elute Cd. It was evident that during the loading and washing steps, the Cd was retained on the column and only the Rh and Ag were eluted.

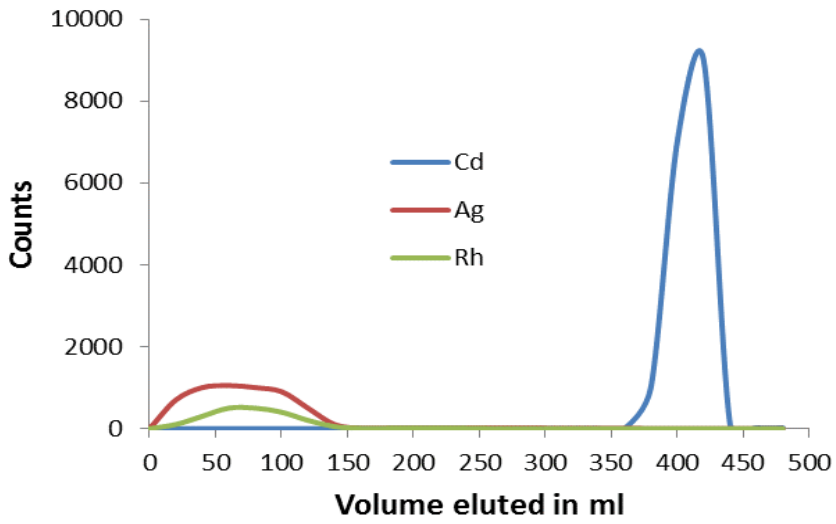

Figure 12: Elution curve for Cd, Ag and Rh on AG1-X10 resin column (length 6 cm & inner diameter 1.5 cm) with eluents 2 M HCl (365 mL) for Ag and Rh and 1 M HNO_3 (100 mL) for Cd.

The radionuclide impurities measured by γ-spectrometry are listed in Table 8. The ^{101m}Rh detected in the solution is obtained by decay of ^{101}Pd and this can be produced at a proton beam ≥ 36 MeV. For the hot cell runs, the irradiated Ag target that was located in the low energy window and that was processed with the same experimental conditions to that of preliminary run 4-6 (6 cm x 1.5 cm resin column) had shown consistent results to the preliminary runs 4-6 as shown in Table 9.

Table 7: Preliminary runs of Cd, Rh and Ag column chemical separations

Preliminary run number	**Size column (cm)**	**Cd recovered from the resin column (%)**	**Contaminant in the final product** % Rh	**Contaminant in the final product** % Ag
1	4 x 1.6	94.1	3.0	1.0
2	4 x 1.6	94.1	3.0	1.0
3	5 x 1.5	95.2	2.0	1.0
4	6 x 1.5	99.9	0	0
5	6 x 1.5	99.9	0	0
6	6 x 1.5	99.9	0	0

Table 8: Radionuclide impurities of ^{109}Cd final solution using AG1-X10 / 2 M HCl system

Nuclide	**Half-life**	**Energy, KeV**	**Counts 1 m slit**	
			Original	**Final**
^{101g}Rh	3.2 y	127.0 (70 %)	238.0	ND
^{101m}Rh	4.34 d	306.86 (87 %)	ND	ND
^{105}Ag	41.29 d	344.52 (41.4 %)	542.0	ND
^{109}Cd	462 d	88.0 (3.6 %)	6890.0	6830.0

ND: not detected

Table 9: Hot runs of Cd, Rh and Ag column chemical separations

Hot run number	**^{109}Cd final product**	**Contaminant in the final product % Rh**	**Contaminant in the final product % Ag**	**Total irradiation time on target (mins)**	**^{109}Cd activity at end of the bombardment (mCi)**
1	>99.99	0	0	10 [a]	0.0200
2	>99.99	0	0	30 [b]	0.0612
3	>99.99	0	0	60 [c]	0.123

Standard deviation: 0.022±0.001a; 0.066±0.000b; 0.123±0.002c. Values are mean ± standard deviation (n=2). Means with different letters within same column are significantly different ($p<0.05$)

The recovery of ^{109}Cd from the AG1-X10 resin column was >99 % and no Rh or Ag radionuclide contaminants were detected in the final product. The irradiation time of the Ag target for the 3 runs ranged between 10 and 60 minutes and this yielded a consistent yield of ^{109}Cd at 0.0019 mCi / μAh at end of bombardment (projected from data at the end of separation).

CHAPTER 3: CONCLUSION

The production of ^{103}Pd and ^{109}Cd was achieved by irradiating the tandem ^{nat}Ag/^{nat}Ag target using a 66 MeV proton beam of Separated Sector Cyclotron of iThemba LABS. The irradiation of a tandem Ag/Ag targets arrangement had provided us with an opportunity to produce the bulk ^{103}Pd and ^{109}Cd simultaneously in one irradiation arrangement. During this arrangement, the target with in the higher energy slot produced ^{103}Pd while the target in the low energy produced ^{109}Cd. By this target arrangement, the irradiation time was increased two fold to produce ^{103}Pd and ^{109}Cd as compared to when ^{103}Pd and ^{109}Cd was produced separately (non-simultaneously) with single targets at separate irradiation times.

The radiochemical separation of ^{103}Pd and ^{109}Cd from the tandem ^{nat}Ag/^{nat}Ag targets was achieved in two separate chemical processes using ion exchange chromatographic techniques (Chelex-100 and AG 1-X10 resins). During the chemical separation of ^{103}Pd, we were able to reduce the chemical processing from a double column separation (previous work) to a single Chelex 100 column separation (13 cm x 1 cm). The Ag targets that were irradiated had shown a 100% retention of the Pd radionuclides during the loading step and when the final product was eluted no Ag radionuclides were found, except for Rh radionuclides at levels of <1% in the final product. For the three hot cell runs, the production of ^{103}Pd was consistent at 1.5 mCi / µAh at the end of bombardment (projected from end of separation data).

During the chemical separation of ^{109}Cd, we were able to improve on the quality and the activity yield of the previous work by just increasing the column length of the AG1-X10 resin column (6 cm x 1.5 cm) and increasing the amount of Cu turnings to ensure complete reduction of the Ag. The recovery of ^{109}Cd from the AG1-X10 resin column was >99% and no Rh or Ag radionuclide contaminants were found in the final product. For the four hot cell

runs, the production of ^{109}Cd was consistent at 0.0019 mCi / µAh at the end of bombardment (projected from end of separation data). In conclusion, the results of this investigation represent a new opportunity for the production of ^{103}Pd and ^{109}Cd using a tandem ^{nat}Ag/^{nat}Ag targets. The results of this investigation have since been published [91].

Future research extending from this investigation is expected to include the following:

- To produce bulk ^{103}Pd and ^{109}Cd radionuclides at routine production levels that satisfy market demand.

- To explore the possibility to produce a ^{103}Pd/^{103m}Rh *in vivo* generator system for medical application by combining ^{103}Pd and ^{103m}Rh into one radiopharmaceutical. ^{103m}Rh is a target radiation therapy of small neuroendocrine tumours.

- To produce a ^{109}Cd/^{109m}Ag generator system from our ^{109}Cd product for uses of venogram and angiogram as an alternative to other biomedical generators of ultra-short lived gamma emitters.

CHAPTER 4: REAGENTS AND EQUIPEMENT

Analytical grade reagents were used throughout this work and were obtained from Merck (SA) Pty. Ltd. or Sigma Aldrich GmbH. The Chelex-100 chelating resin (100-200 mesh, in Na^+ form) and AG1-X10 anion exchange resins (100-200 mesh, in Cl^- form) were obtained from Bio-Rad Laboratories, Richmond, USA. Cu turnings were obtained from BDH (B.D.H. Laboratory Chemicals Group, England). Deionised water was obtained from an on-site Millipore MilliQ reagent grade water system which had produced a conductivity of greater than 1.8 $M\Omega\,cm^{-1}$. Modified polyethylene syringes were used as columns. The peristaltic pump was used in order to maintain the solution's speed during its load to the column. To determine the radioactivity of each radionuclide, the standard off-line γ-ray spectrometer with a high purity germanium (HPGe) detector was used. The detector was shielded from the background radiation by a lead cylinder with an inner layer of copper to reduce gamma-ray scattering. An HPGe detector used was accurately calibrated with standardized calibration sources for both efficiency and energy. The detector has a relative efficiency of 10.1% and a resolution of 3.18 KeV FWHM at 1.3 MeV. The photo-peak areas are determined by means of the quantitative Canberra Genie 2000 analysis software in conjunction with a Canberra DSA 1000 multi-channel analyzer system.

CHAPTER 5: EXPERIMENTAL

5.1 PREPARATION OF ^{nat}Ag/^{nat}Ag TARGETS

The method used for the production of ^{103}Pd and ^{109}Cd involves the irradiation of two natural silver targets (^{nat}Ag), in tandem, with use of the entire 66 MeV primary proton beam from the Separated Sector Cyclotron (SSC) of iThemba LABS. The tandem ^{nat}Ag/^{nat}Ag was irradiated in the horizontal beam target station vault of the Radionuclides Production Department at a current of 65 μA.

For the preparation of appropriate tracers, the Ag/Ag targets were irradiated for 10 mins and for hot cell production work the target was irradiated for 10- 60 mins. Targets discs of 2 cm in diameter with a mass of 9 g were made from a high purity metallic silver rod, 99.999%. The target disc was enclosed in an aluminum capsule. The targets were 3 mm thick and had 1 mm of cooling water on each side for cooling purposes. The tandem targets were placed in the high energy slot and low energy slot to produce the bulk ^{103}Pd and ^{109}Cd, respectively.

The targets were in direct contact with the cooling water (50 L/min flow rate) inside the aluminum target holder. The energy region for the production of ^{103}Pd was 62.515 MeV – 40.173 MeV and for ^{109}Cd was 38.652 MeV – 0 MeV. The targets are irradiated outside the beam line vacuum, from which they are isolated by means of a double-foil beam window assembly. The helium cooling system was developed to provide cooling for beam window foils, by means of forced convection of helium between the two foils, and for target components that require helium. The thickness of helium layer was 10.0 mm. Figure 17 shows the target holder configuration which highlights the make-up of the target holder, the cooling system and the beam direction.

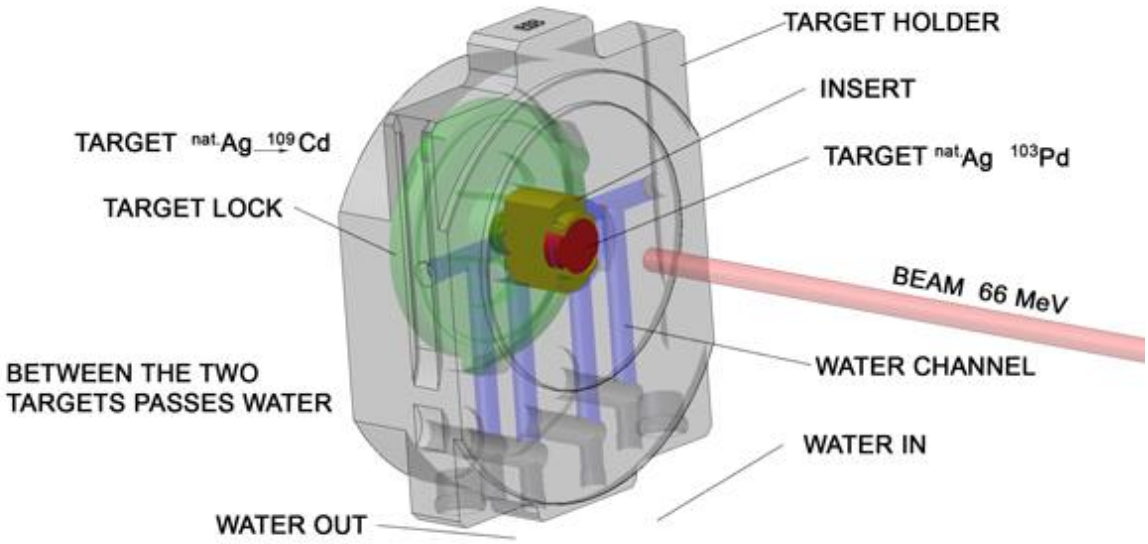

Figure 17: Configuration of target holder

5.2 TARGET DISSOLUTION

5.2.1 Ag target for ^{103}Pd

The irradiated silver disk that was placed in the high energy slot was removed from the aluminium capsule and washed with deionized water to remove any surface impurities. The target was transferred to a beaker containing 50 mL concentrated HNO_3 and was dissolved under a low heat (50 $^{\circ}$C) for one hour. On complete dissolution, the solution was evaporated to dryness and the residue was dissolved in 225 mL 0.4 M HNO_3. After cooling, 0.028 g $Pd(NO_3)_2$ was added to the resultant solution. The solution was now ready for further column purifications.

5.2.2 Ag target for ^{109}Cd

The irradiated silver disk that was placed in the low energy slot was removed from the aluminium capsule and washed with deionized water to remove any surface impurities. The target was transferred to a beaker containing 50 mL concentrated HNO_3 and was dissolved under low heat (50 $^{\circ}$C) for two hours. On complete dissolution, the solution was evaporated to dryness and the residue was dissolved in 40 mL of deionised water and this was repeated twice for further dilution to ensure that the pH of the solution is kept between 2 and 7. Deionised water (50 mL) was added to the residue which was evaporated to dryness, 30 to 35 g of Cu turnings were then added to the solution and the mixture was stirred for one hour. The resultant solution was decanted into a 50 mL syringe that contained glass fibre at the bottom to ensure filtration of the reduced Ag deposited on the Cu turnings and excess Cu. The precipitate was washed twice with 30 mL of deionized water and the washings were decanted into the syringe. The combined filtrates were treated with 15 mL of 30% hydrogen peroxide and the resultant solution was evaporated to dryness. The residue was reconstituted in 100 mL of 2 M HCl containing 5 mL of hydrogen peroxide (30%). The solution was now ready for further column purifications.

5.3 PREPARATION OF RESINS

A desired quantity of resin was placed in a polyethylene bottle with deionized water and stirred for 24 h to ensure complete hydration. On completion, the supernatant was decanted and fresh deionized water was added to wash the resin (this was repeated 5 times). The resin was now ready for the preparation of the appropriate columns. Generally an appropriate size syringe is filled with a slurry of resin which has a 60 μm sinter (frit) at the top and bottom

section of the syringe with a Teflon plunger to seal it off. The sealed resin syringe, now resin column, is ready to be equilibrated with the appropriate solution.

5.4 SEPARATION OF ^{103}Pd FROM Ag AND Rh

In the preliminary work four column sizes (Column A = length 3 cm & inner diameter 1 cm, Column B = length 16 cm & inner diameter 1.5 cm, Column C = length 11 cm & inner diameter 1 cm, Column D = length 13 cm & inner diameter 1 cm) were investigated using the Chelex 100 resin. Pd, Rh and Ag radionuclide tracers was obtained from a Ag target that was irradiated for 10 min and dissolved as described in 3.1.2.1. Precise aliquots (50 mL) of this bulk tracers solution were used to track the separation efficiency of the chemical process. In each case, 10 mL of the Pd, Rh and Ag tracers was added to the solution.

5.4.1 Preliminary Case 1

A 9 g disk of silver was dissolved as described in 3.1.2.1. To the solution, were added radiotracers Pd, Rh and Ag and mixed by stirring for 5 min. The resultant solution was passed through the Chelex 100 column (Column A) that was previously equilibrated with 50 mL 1 M HNO_3. After completion of the loading step, the column was washed with 100 mL of 1 M HNO_3 to remove the trace of Ag and Rh radionuclides. To remove the Pd radionuclides, 100 ml of 10 M HCl was used. The peristaltic pump speed was at 1 mL / min throughout.

5.4.2 Preliminary Case 2

A 9 g Ag disk was dissolved as described in 3.1.2.1. To the dissolved solution, radiotracers Pd, Rh and Ag were added and mixed by stirring for 5 min. The resultant solution was passed

through the Chelex 100 column (Column B) that was previously equilibrated with 50 mL 1 M HNO_3. After completion of the loading step, the column was washed with 100 mL of 1 M HNO_3 to remove the trace amounts of Ag and Rh radionuclides. To remove the Pd radionuclides, 100 ml of 10 M HCl was used. The peristaltic pump speed was 1 mL / min throughout.

5.4.3 Preliminary Case 3

A 9 g Ag disk was dissolved as described in 3.1.2.1. To the dissolved solution, radiotracers Pd, Rh and Ag were added and mixed by stirring for 5 mins. The resultant solution was passed through the Chelex 100 column (Column C) that was previously equilibrated with 50 mL 1 M HNO_3. After completion of the loading step, the column was washed with 100 ml of 1 M HNO_3 to remove the trace amounts of Ag and Rh radionuclides. To remove the Pd radionuclides, 100 mL of 10 M HCl was used. The peristaltic pump speed was at 1 mL / min throughout.

5.4.4 Preliminary Case 4

A 9 g disk was dissolved as described in 3.1.2.1. To the dissolved solution, radiotracers Pd, Rh and Ag were added and mixed for 5 mins. The resultant solution was passed through the Chelex 100 column (Column D) that was previously equilibrated with 50 mL 1 M HNO_3. After completion of the loading step, the column was washed with 100 mL of 1 M HNO_3 to remove the trace amounts of Ag and Rh radionuclides. To remove the Pd radionuclides, 100 ml of 10 M HCl was used. The peristaltic pump speed was at 1 mL / min throughout.

To confirm the purification ^{103}Pd from Ag and Rh radionuclides, the conditions used in preliminary 4 was used to develop an elution curve. 20 ml fractions were taken of the loading

step, washing step and eluting step and was measured with a high purity germanium (HPGe) detector.

5.4.5 Hot Run

The irradiated 9 g Ag disk was dissolved as described in 3.1.2.1. The resultant solution was passed through a Chelex 100 column (Column D) that was previously equilibrated with 50 mL of 1 M HNO_3. After completion of the loading step, the column was washed with 100 mL of 1 M HNO_3 to remove the trace amounts of Ag and Rh radionuclides. To remove the Pd radionuclides, 100 mL of 10 M HCl was used. The eluate was collected and evaporated to dryness and the ^{103}Pd was dissolved with 30 mL of deionized water and evaporated (repeated twice). The final product was picked up with 5 mL 0.5 M HNO_3. The peristaltic pump speed was 1 mL / min throughout.

5.5 SEPARATION OF ^{109}Cd FROM Ag AND Rh

In the preliminary work three column sizes (Column A = 4 cm & inner diameter 1.6 cm, Column B = 5 cm & inner diameter 1.5 cm, Column C= length 6 cm & inner diameter 1.5 cm) was investigated using the AG1-X10 resin for the separation of ^{109}Cd from ^{nat}Ag target.

5.5.1 Preliminary case 1- 2

A 9 g Ag disk was dissolved as described in 3.1.2.2. To the dissolved solution, radiotracers Pd, Rh and Ag were added and mixed by stirring for 5 min. The resultant solution was passed through a AG1-X10 resin column (Column A) that was previously equilibrated with 100 mL 2 HCl. After completion of the loading step, the column was washed with 250 mL of 2 M

HCl to remove the trace amounts of Cu^{2+}, Cu^{+} and Rh radionuclides. The Cd was removed from the column using 100 mL of 1 M HNO_3. The peristaltic pump speed was 1 mL / min throughout.

5.5.2 Preliminary Case 3

A 9 g Ag disk was dissolved as described in 3.1.2.2. To the dissolved solution, radiotracers Pd, Rh and Ag were added and mixed by stirring for 5 min. The resultant solution was passed through a AG1-X10 resin column (Column B) that was previously equilibrated with 100 mL 2 M HCl. After completion of the loading step, the column was washed with 250 mL of 2 M HCl to remove the trace amounts of Cu^{2+}, Cu^{+} and Rh radionuclides. The Cd was removed from the column using 100 mL of 1 M HNO_3. The peristaltic pump speed was 1 mL / min throughout.

5.5.3 Preliminary Case 4 - 6

A 9 g Ag disk was dissolved as described in 3.1.2.2. To the dissolved solution, radiotracers Pd, Rh and Ag were added and mixed by stirring for 5 min. The resultant solution was passed through a AG1-X10 resin column (Column C) that was previously equilibrated with 100 mL 2 HCl. After completion of the loading step, the column was washed with 250 mL of 2 M HCl to remove the trace amounts of Cu^{2+}, Cu^{+} and Rh radionuclides. The Cd was removed from the column using 100 mL of 1 M HNO_3. The peristaltic pump speed was 1 mL / min throughout. To confirm the purification of ^{109}Cd from the Ag and Rh radionuclides, the conditions used in preliminary 4-6 was used to develop an elution curve. 20 ml fractions were taken of the loading step, washing step and eluting step and was measured with a high purity germanium (HPGe) detector.

5.5.4 Hot Run

The irradiated 9 g Ag disk was dissolved as described in 3.1.2.2. After the dissolution of the target, the resultant solution was passed through a AG1-X10 resin column (Column C) that was previously equilibrated with 100 mL 2 M HCl. After completion of the loading step, the column was washed with 250 mL of 2 M HCl to remove the trace amounts of Cu^{+}, Cu^{2+} and Rh radionuclides. The Cd was removed from the column using 100 mL of 1 M HNO_3. The solution was evaporated to dryness and reconstituted in 5 mL 0.5 M HNO_3. The peristaltic pump speed was 1 mL / min throughout.

REFERENCES

1. M. F. l'Annunziata, in *Handbook of Radioactivity Analysis*, Elsevier, Oxford, UK, 3rd edn., 2012, pp. 1-162.
2. M. F. L'annunziata, W. Burkart, in *Radioactivity: Introduction and History*, Elsevier, The Netherlands, 2007, pp. 1-70
3. M.C. Malley, in *Radioactivity: A History of a Mysterious Science*, Oxford University Press, USA, 2011, pp. 3-82.
4. B. Skwarzec, *Anal. Bioanal. Chem.*, 2011, **400**, 1547-1554.
5. K. H. Lieser, in *Nuclear and Radiochemistry: Fundamentals and Applications*, Wiley, New York, (USA), 1st edn, 1997, pp. 475.
6. G.R. Choppin, J.O. Liljenzin, J. Rydberg, in *Radiochemistry and Nuclear Chemistry*, Butterworth-Heinemann, USA, 3rd edn., 2002, pp. 704.
7. E. Rutherford, J. Chadwick, C.D. Ellis, in *Radiations from Radioactive substances*, Cambridge University Press, UK, 1951, pp. 1-7.
8. A. Debierne, *C.R. Acad. Sci. Paris*, 1900, **130**, 906.
9. A. Debierne, *C.R. Acad. Sci. Paris*, 1900, **129**, 593.
10. G.B. Saha, in *Physics and Radiobiology of Nuclear Medicine*, Springer, 3rd edn., 2006, chap. 5, pp. 44-49.
11. K.H. Lieser, in *Nuclear and Radiochemistry: Fundamentals and Applications*, John & Sons, Inc., New York, 2nd edn., 2001, pp. 467.
12. M.M.D.M. Shehata, PhD Thesis, der Universitätzu Köln: uasKairo, 2011.
13. M.J. Welch, C.S. Redvanly, in *Handbook of Radiopharmaceuticals: Radiochemistry and Applications*, John Wiley & Sons, Inc., New York, 2002, pp. 862.
14. G. Stocklin, S.M. Qaim, F. Rosch, *Radiochim. Acta*, 1995, **70/71**, 249-272.
15. H.C. Urey, F.G. Brickwedde, G.M. Murphy, *Phys. Rev.*, 1932, **40**, 1-15.

16. E.O. Lawrence, M.S. Livingston, *Phys. Rev.*, 1931, **38**, 834-834.

17. www.sasnm.co/nuclear-medicine-in-sa.aspx [accessed: 20/01/2014]

18. C. Naidoo, International Workshop on Positron Studies of Defects PSD-11, 29.8.-2.9.2011, Delft, Netherlands.

19. I.A. Abbasi, *PhD Thesis*, QUAID-I-AZAM University: Islamabad, 2005.

20. A.R. Jalilian, M. Sadeghi, Y.Y. Kamrani, A. Bahrami, *Iran. J. Radiat. Res.*, 2006, **4**, 41-47.

21. M. Sadeghi, B. Shirazi, *Appl. Radiat. Isot.*, 2008, **66**, 1810-1813.

22. M. Sadeghi, H. Afarideh, R. Gholamreza, P. Van der Winkel, *Radiochim. Acta*, 2006, **94**, 217-221.

23. M. Faßbender, F.M. Nortier, I.W. Schroeder, T.N. Van Der Walt, in *Proceedings of the Eight Workshop on the Targetry and Target Chemistry*, St Louis: MO, 1999, pp 1-2.

24. International Atomic Energy Agency, *Utilization Related Design Features of Research Reactors: A Compendium*, IAEA: Vienna, Austria, STI/DOC/010/455, 2007.

25. International Atomic Energy Agency, *Nuclear Data for the Production of Therapeutic Radionuclides*, IAEA: Vienna, Austria, STI/DOC/010/473, 2011.

26. M. Hussain, S. Sudar, M.N. Aslam, H.A. Shah, R. Ahmad, A.A. Malik, S.M.Qaim, *Appl. Radiat.Isot.*, 2009, **67**, 1842-1854.

27. M. Hussain, *PhD Thesis*, Government College University Lahore: Lahore, 2009.

28. J. A. O'Donoghue, T. E. Wheldon, *Phys. Med. Biol.*, 1996, **41**, 1973–1992.

29. S. Sudár, F. Cserpak, S.M.Qaim, *Appl. Radiat. Isot.*, 2002, **56**, 821-831.

30. I. Silverman, E. Lavie, A. Arenshtam, D. Kijel, D. Vaknin, M.Veinguer, A. Nagler, *Nucl. Instrum. Methods Phys. Res., Sect. B*, 2007, **261**, 747-750.

31. M.S. Uddin, M. Hagiwara, M. Baba, F.Tarkanyi, F. Ditroi, *Appl. Radiat. Isot.*, 2005, **62**, 533-540.

32. International Atomic Energy Agency, *Production techniques and quality control of sealed radioactive sources of palladium-103, iodine-125, iridium-192 and ytterbium-169*, Final report of a coordinated research project 2001–2005, IAEA-TECDOC-1512, IAEA: Vienna, 2006.

33. A.R. Jalilian, Y.Y. Kamraniand M. Sadeghi, *Nukleonika*, 2006, **51**, 119-123.

34. F. Abboud, P. Scalliet, S. Vynckier, *Med Phys*., 2008, **35**, 5841-5850.

35. Z. Chunfu, W. Yongxian, Z. Yongping, Z., Xiuli, *Appl. Radiat. Isot.*, 2001, **55**, 441-445.

36. International Atomic Energy Agency, *Cyclotron Produced Radionuclides: Physical characteristics and Production methods*, IAEA: Vienna, Austria, 2009.

37. M. Sadeghi, H. Karami, P. Sarabadani and F. Bolourinovin, *J. Radioanal. Nucl. Chem*., 2009, **281**, 619-673.

38. L.O. Landini and J.A. Osso Jr., *J. Radioanal. Nucl. Chem.*, 2001, **250**, 429–431.

39. M. Sadeghi, P. Sarabandi, H. Karami, *J. Radioanal. Nucl. Chem.*, 2010, **283**, 297-303.

40. M. Faßbender, F.M. Nortier, D.R. Phillips, V.T. Hamilton, R.C. Heaton, D.J. Jamriska, J.J. Kitten, L.R. Pitt, L.L. Salazar, F.O. Valdez and E.J. Peterrson, *Radiochim. Acta*, 2004, **92**, 237-243.

41. M. Mirzaii, M. Sadeghi, Z. Gholamzadeh, *Iran. J. Radiation. Res*., 2009, **6**, 201-206.

42. R. Van Ammel, S. Pommé, J. Paepen, G. Sibbens, *Appl. Radiat. Isot.*, 2011, **69**, 785-789.

43. I.E. Alekseev, V.V. Lazarev, *Radiochem.*, 2010, **52**, 449-450.

44. M. Sadeghi, M., Mirazaee, Z. Gholamzadeh, A. Karimian and F.N. Bolouri, *Radiochim.Acta*, 2009, **97**, 113-116.

45. K. Aardaneh, C. Naidoo, G.F. Steyn, *J. Radioanal. Nucl. Chem.*, 2008, **276**, 831-834.

46. S. Khujaev, A. Vasidov, E.A., Markelova, *The possibility of obtain radionuclide ^{109}Cd at nuclear reactor*, Institute of Nuclear Physics of AS RUz, Tashkent, Uzbekistan, 2008.

47. Z. Gholamzadeh, M. Sadeghi, M. Mirzaee and M. Aref, *Kerntechnik*, 2011, **76**, 273-276.

48. M. Mirzaee, M. Sadeghi, Z. Gholamzadeh, S. Lahouti, *J. Radioanal. Nucl. Chem.*, 2008, **277**, 645-650.

49. M. Sadeghi, M. Mirzaii, Z. Gholamzadeh, P. Sarabadani, A. Sattari, *Radiochem.*, 2010, **52**, 565-568.

50. J.M. Hutchinson, S.B. Garfinkel, *Int. J. Appl. Radiat. Isot.*, 1971, **22**, 405-14.

51. H. Xiaolong, Y. Shenggui, D. Chunsheng, *Nucl. Instrum. Methods Phys. Res.*, Sect. A, 2010, **621**, 443-446.

52. http://www.Isotopes.Gov/Sites/Production.Html, [accessed on 25/04/2013].

53. A. Hermanne, M. Sonck, A. Fenyvesi, L. Daraban, *Nucl. Instrum. Methods Phys. Res., Sect. B,* 2000, **170**, 281-292.

54. Y.T. Petrusenko, A.G. Lymar, L.I. Nikolaichuk, T.A. Ponomarenko, A.I. Tutubalin, A.G. Shepeler, *Nucl. Phys. Invest.*, 2009, **52**, 60-63.

55. US Pantent 006143431 A (2000).

56. A. Hermanne, M.Sonck, S.Takacs, F.Tarkanyi, Y.Shubin, *J. Nucl. Sci. Technol.*, 2002, **suppl. (2)**, 1286-1289.

57. Ye. Skakun, S.M. Qaim, *Appl. Radiat. Isot.*, 2008, **66**, 653-667.

58. L.F. Mausner, K.L. Kolsky, V. Awasthi, S.C. Srivastava, *J. Label. Cpd. Radiopharm.*, 2001, **44**, s775-s777.

59. M. Faβbender, F.M., Nortier, Schroeder, T.N. Van Der Walt, *Radiochim. Acta*, 1999, **87**, 87-91.

60. K. Aardaneh, H.G. Raubenheimer, T.N. Van der Walt, C. Vermeulen, *J. Radioanal. Nucl. Chem.*, 2003, **256**, 31-35.

61. E.V. Lapshina, V.M. Kokhanyuk, B.L. Zhuikov, G.V. Myasoedova, E.A. Zakhartchenko, D.R. Phillips, D.J. Jamriska, *Report of the International conference on the "Separation of ionic solutes"* Podbanske, High Tartas, Slovakia, September 6-11, 2003.

62. F. Tárkányi, A. Hermanne, B. Király, S. Takács, F. Ditrói, J. Csikai, A. Fenyvesi, M.S. Uddin, M. Hagiwara, M. Baba, T. Ido, Yu. N. Shubin, A.V. Ignatyuk, *Appl. Radit. Isot.*, 2009, **67**, 1574-1581.

63. M.P. Anikina, A.G. Beda, A.V. Davydov, M.M. Korotkov, G.M. Kukavadze, L.Ya. Memelova, *Atomnaya Energiya*, 1987, **62**, 415-417.

64. S. Lahiri, B. Mukhopadhyay, M. Nandy, and N.R. Das, *J. Radioanal. Nucl. Chem.*, 1997, **224**, 155-158.

65. M.S. Mansur, A.Mushtaq, A. Muhammad, *J. Radioanal. Nucl. Chem., Lett.*, 1998, **201**, 205-211.

66. N.N. Krasnov, Yu.G.Sevastjanov, *Int. J.Appl. Radiat. Isot.*,1979, **30**, 783-784.

67. M. Maiti, K. Ghosh, and S. Lahiri, *J. Radioanal. Nucl. Chem.*, 2013, **295**, 1945–1950.

68. F. Tárkányi, B.Király, F. Ditrói, S. Takács, J. Csikai, A. Hermanne, M.S. Uddin, M. Hagiwara, M. Baba, T.Ido, Yu. N. Shubin, S.F. Kovalev, *Nucl. Instrum. Methods Phys. Res., Sect. B,* 2006, **245**, 379-394.

69. Ku, T.H, Hsieh, R.H., Stang, L.G., Richards, Jr.R., Singh, P.P., and Ward, T.E., *Excitation function measurements of proton induced reactions on rhodium and indium: yields of Ru-97, Tc-96, Cd-109, and Sn-113*, 1978, p. 117-118.

70. Smith-Jones, P.M., Strelow, F.W.E., Haasbroek, F.J. Bohmer, R.G, *Applied Radiation and Isotopes*, 1988, **39**, 1073-1078.

71. F. Guerra, M. Leone, N. Robotti, *Phys. Perspective*, 2012, **14**, 33-58.

72. G.C Loventhal and P.L. Airey, in *Practical Applications of Radioactivity and Nuclear Radiations*, Cambridge University Press, USA, 2004, pp 181-267.

73. International Energy Atomic Agency, *Nuclear Technology Review*, Austria, 2012.

74. J. Magill, J. Galy, in *Radioactivity • Radionuclides • Radiation*, Springer, Karlsruhe, 2005, pp 266.

75. D.W. Loveland, D.J. Morrissey, J.T. Seaborg, in *Modern Nuclear Chemistry*, John Wiley & Sons, New Jersey, 2006, pp 707.

76. S. Sahoo, S. Sahoo, *Phys. Educ.*, 2006, 5-11.

77. WISE/ NIRS Nuclear Monitor, in *Medical Radioisotopes Production Without A Nuclear Reactor*, 2010, **N^0 710/711**, 1-24.

78. International Atomic Energy Agency, *Cyclotron Produced Radionuclides: Principles and Practice*, IAEA: Vienna, Austria, 2008, Chap. 2, pp. 7-29.

79. A. Braithwaite, F.J. Smith, in *Chromatographic method*, Kluwer academic, Dordrecht, the Netherlands, 5th edn., 1996, pp. 571.

80. R.G. Bennett, in *Markets for reactor-produced non-fission radioisotopes*, US department of energy, IDAHO national engineering laboratory, 1995.

81. M. Naushad, *Ion Exchange Lett.*, 2009, **2**, 1-14.

82. Dr. Inamuddin, L. Mohammad, in *Ion Exchange Technology I: Theory and Materials*, Springer, Dordrecht Heidelberg, 2012, pp 211-298.

83. A.A. Zagorodhi, in *Ion Exchange Materials Properties and Applications*, Elsevier, Amsterdam, 1st edn., 2007, pp. 9-54.

84. M. Maiti, S. Lahiri, B.S. Tomar, *J. Radioanal. Nucl. Chem.*, 2011, **288**, 115-119.

85. Y. Dardenne, K.J. Rengan, *Radioanl. Nucl. Chem.*, 1987, **116**, 355-363.

86. Z. Samczynski, B. Danko, R. Dybczynski, Investigations on possibilities of determination of some precious metals in geological and environmental smples by

neutron activation analysis. Annual Report of Institute of Nuclear Chemistry and Technology, 1998, PL9902232: 100-101

87. R.N. Ceo, M.R. Kazerouni, K. Rengan, *J. Radioanal. Nucl. Chem.*, 1993, **172**, 43-48.

88. K.A. Kraus, F. Nelson, *Anion exchange studies of the fission products* In: Proceedings of the 1st International Conference on Peaceful Uses of Atomic Energy, Geneva Vol. 7, 1956, 113–125. A/CONF.8/7, United Nations Publishers, New York

89. N. Saito, *Pure & Appl. Chem.*, 1984, **56**, 523-539.

90. J.P. Faris, R. F. Buchanan, *Anal. Chem.*, 1964, **36**, 1157-1158.

91 C. Ineza, C. Naidoo, C. Vermeulen, J. Mphahlele, *J. Radioanal. Nucl. Chem.*, 2014, **301**, 227-236.

92. G.F. Steyn, C. Vermeulen, A.H. Botha, J.L. Conradie, J.P.A. Crafford, J.L.G. Delsink, J. Dietrich, H. du Plessis, D.T. Fourie, Z. Kormány, M.J. van Niekerk, P.F. Rohwer, N.P. Stodart, J.G. de Villiers, *Nucl. Instrum. Methods Phys. Res.*, Sect. A, 2013, **727**, 131–144.

APPENDIX

1: BOMBARDMENT FACILITIES FOR RADIONUCLIDE PRODUCTION AT iThemba LABS

A total of four high-energy beamlines are currently dedicated to the radionuclide production programme at iThemba LABS—three horizontal beam lines in one vault and one vertical beam line in another.

1.1 Horizontal Beam Target Station (HBTS)

The first horizontal beam target station built at iThemba LABS, in 1988, referred to as Target Station 1 and often also by its nickname "*The Elephant*", is a facility for the bombardment of batch targets. The robot arm, transport trolley and part of the rail are shown in Figure 13. The targets are irradiated outside the beamline vacuum, from which they are isolated by a helium-cooled double-foil beam window and the cooling water is supplied to the targets through a pneumatic pusher arm. It is used to produce the mainly five "bread and butter" radionuclides ^{22}Na, ^{67}Ga, ^{68}Ge, ^{82}Sr and ^{123}I and a variety of radionuclides for experimental purposes like ^{44}Ti, ^{55}Fe, ^{64}Cu, ^{103}Pd, ^{133}Ba, ^{109}Cd, ^{139}Ce and ^{227}Pa. Beams of 66 MeV protons and intensities up to 100 μA are routinely used in this facility.

A second target station, dedicated to the bombardment of semi-permanent targets, was designed and built at iThemba LABS. Target Station 2, usually referred to by its nickname "*Babe*", received first beam in 1996. It is also a shielded and electrically isolated station like Target Station 1 but slightly smaller as shown in Figure 14. This target station is used for the

production of ^{18}F using ^{18}O-water. The main difference is the absence of the robot arm for target exchanges.

The third beamline in the horizontal-beam vault is dedicated to experimental studies. We would like to mention it here for the sake of completeness, in particular since it has been equipped with a specialized target station for the activation of thin targets and/or foil stacks with beams of low intensity.

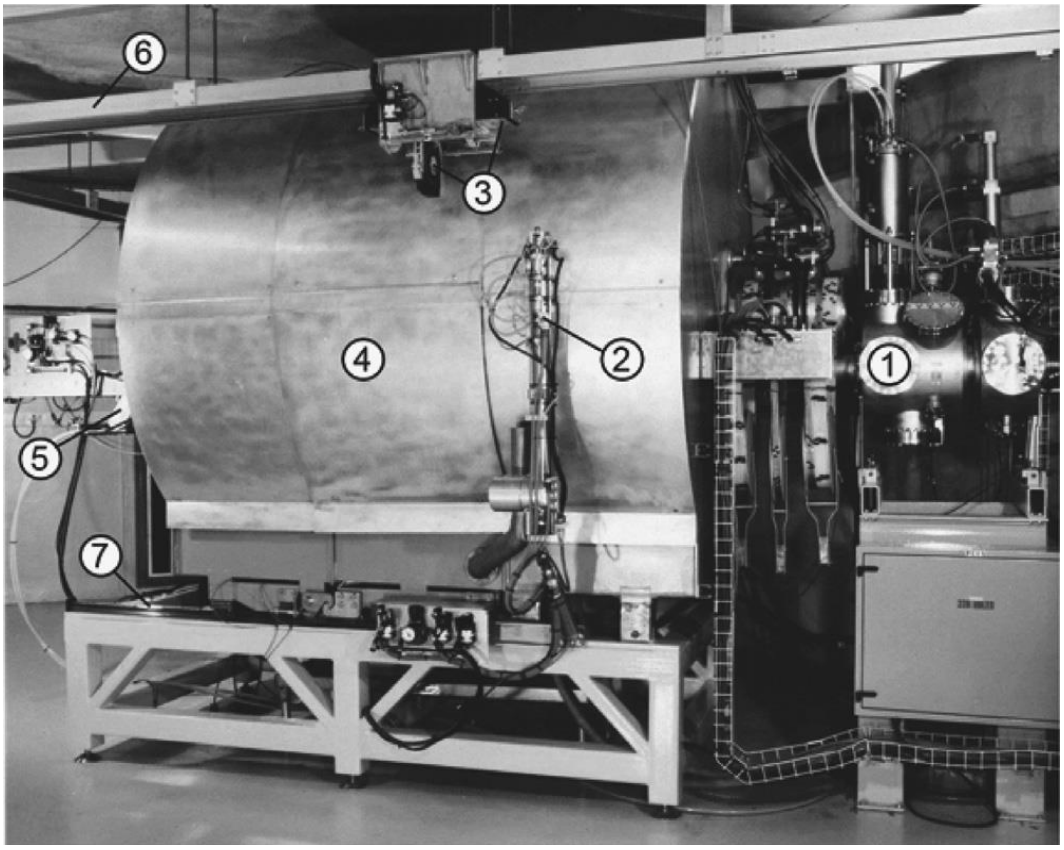

Figure 13: Target station 1 for irradiating batch targets, showing (1) the last diagnostic chamber on a horizontal beamline, (2) robot-arm for target exchanges, (3) a target holder on a target transport trolley, (4) local radiation shield, (5) pusher arm to connect cooling water, (6) rail for target transport, and (7) rail on which part of the shielding can move in order to open the station [92].

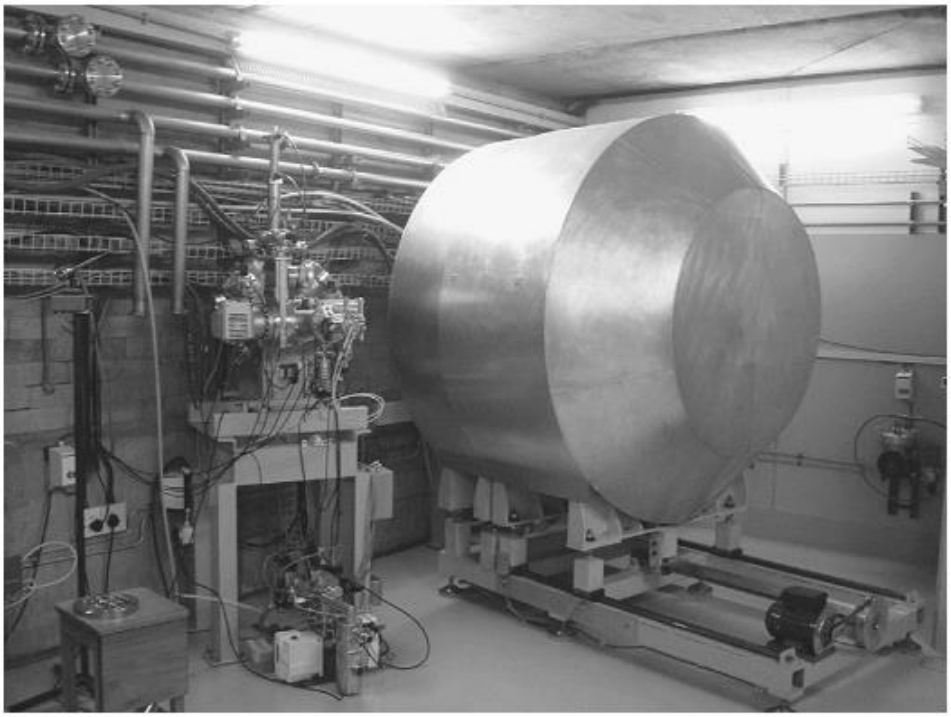

Figure 14: Target station for irradiating semi-permanent targets [92].

1.2 Vertical Beam-line Target Station (VBTS)

The vertical-beam target station (VBTS) was specifically designed for the production of longer-lived radionuclides with increased beam intensities. It is currently used for the large-scale production of ^{22}Na, ^{68}Ge and ^{82}Sr with beam currents of typically 250μA, but bombardments up to 300μA have been demonstrated. A photograph of the VBTS is shown in 15.

Common to both the Elephant and the VBTS is beam sweeping, in order to enlarge the area of the target directly exposed to the beam while the main difference between them, other than the direction of the beam being vertical, is the omission of a target magazine.

Figure 15: An overall view of the VBTS, a bombardment station for the irradiation of batch targets utilizing a vertical proton beam. The station is showed with the radiation attenuation shield closed. The remotely-controlled pneumatic robot arm which facilitates target transfers is shown in the foreground, while the electrified rail for target transport can be seen in the background. Note the beam diagnostics chamber on top of the target station [92].

2. TARGETRY

Most of the batch targets used at iThemba LABS consist of the target material of choice encapsulated in either aluminium, stainless steel or niobium. The infrastructure to encapsulate target material in aluminium is resident in the laboratory, whereas stainless steel and niobium encapsulation have to be outsourced. The encapsulation serves two purposes: 1) to protect the target material from the cooling water, and 2) to contain the target material, which often goes into a molten state during bombardment with high-intensity beams. The choice of encapsulation material depends on the target material to be contained. Figure 16 shows different target holders and targets in the HBTS.

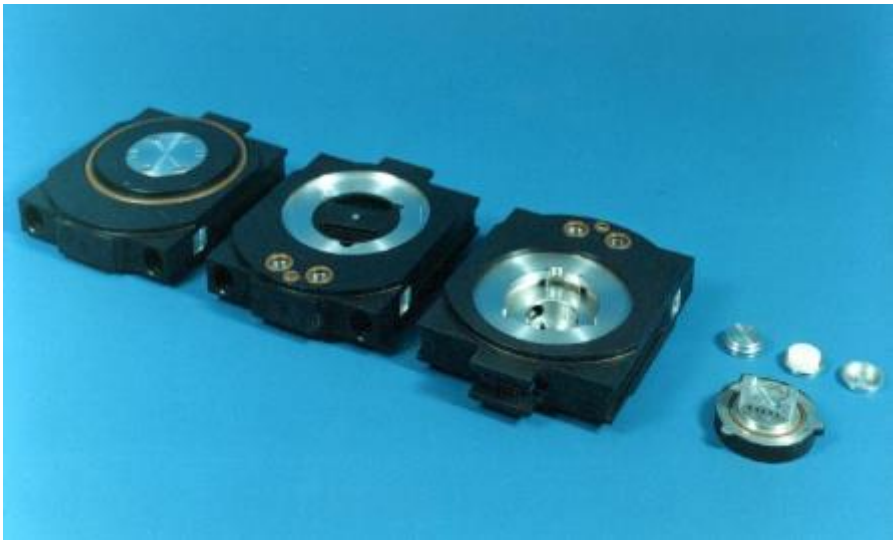

Figure 16: HBTS Targets and Target Holders [18].